

TOPICAL REVIEW • OPEN ACCESS

High performance energy-saving electrocatalysts for hydrogen evolution reaction: a minireview on the influence of structure and support

To cite this article: Chunyan Zuo *et al* 2025 *Mater. Futures* 4 012101

View the [article online](#) for updates and enhancements.

You may also like

- [Hydrogen evolution on non-metal oxide catalysts](#)
Stephen Rhatigan, Marie-Clara Michel and Michael Nolan
- [Advances in theoretical calculations of MXenes as hydrogen and oxygen evolution reaction \(water splitting\) electrocatalysts](#)
Pengfei Hou, Yumiao Tian, Di Jin *et al.*
- [Recent advances of single-atom electrocatalysts for hydrogen evolution reaction](#)
Zhixue Ma, Lijuan Niu, Wenshui Jiang *et al.*

Topical Review

High performance energy-saving electrocatalysts for hydrogen evolution reaction: a minireview on the influence of structure and support

Chunyan Zuo^{1,2,4}, Hengyuan Hu^{3,4}, Meisheng Han^{3,*} , Yejun Qiu^{2,*} and Guohua Tao^{1,*}

¹ School of Advanced Materials, Peking University Shenzhen Graduate School, Shenzhen 518055, People's Republic of China

² Shenzhen Engineering Laboratory of Flexible Transparent Conductive Films, School of Materials Science and Engineering, Harbin Institute of Technology, Shenzhen 518055, People's Republic of China

³ Department of Mechanical and Energy Engineering, Southern University of Science and Technology, Shenzhen 518055, People's Republic of China

E-mail: hanms@sustech.edu.cn, yejunqiu@hit.edu.cn and taogh@pkusz.edu.cn

Received 22 September 2024, revised 23 December 2024

Accepted for publication 5 January 2025

Published 21 February 2025



CrossMark

Abstract

Generating hydrogen from water electrolysis is a promising clean energy strategy that may help alleviate energy crisis, which stimulates tremendous research interests in searching high performance catalysts with low energy consumption. Here, we review recent progresses on the development of high performance electrocatalysts for hydrogen evolution reaction (HER) from the energy consumption perspective. A universal energy label based on energy conversion efficiency (ECE) is proposed to evaluate the HER performance, and a global design strategy incorporating both catalyst and support in the same integrated framework is advocated. In particular, the structural influence on the ECE and the stability of HER electrocatalysts is discussed, and the role of support carriers in forming energy-saving catalytic systems with minimized non-HER energy loss, which are vital for practical processes, is highlighted. This paper provides new insights into the structure-property relationship and the support effect in developing highly efficient and durable electrocatalysts for HER.

Keywords: support, electrocatalyst, hydrogen evolution reaction, iR compensation, long-term stability, energy conversion efficiency

⁴ These authors contributed to this work equally.

* Authors to whom any correspondence should be addressed.



Original content from this work may be used under the terms of the [Creative Commons Attribution 4.0 licence](https://creativecommons.org/licenses/by/4.0/). Any further distribution of this work must maintain attribution to the author(s) and the title of the work, journal citation and DOI.

1. Introduction

The energy issues grow prominently along with the development of human society, and it is desired that the conventional energy resources such as coal, oil and natural gas can be replaced by renewable and sustainable energy resources such as solar energy, wind energy and tidal energy [1–3]. Hydrogen (H_2) is one of perfect green energy carriers with the advantages of zero pollution emission and high energy density, and H_2 from water-splitting via electrocatalysis is an ideal complement to the renewable energy of intermittent characteristics [4]. Thus, the development of high performance electrocatalysts for hydrogen evolution reaction (HER) involved in water-splitting is one of the hot research topics in recent years.

Recent developments on HER electrocatalysts mainly focus on two aspects, i.e. the cost-effective efficiency and the long-term stability. Noble metal platinum (Pt) is an ideal HER catalyst, being able to achieve high current density with a low overpotential, but the scarce reserves on Earth restrict its wide application [5, 6]. The non-noble metal HER catalysts are also attractive and productive. For example, the Nickel (Ni) based catalysts could perform equally well in HER as Pt requiring similar overpotentials at a specific current density [7, 8]. And the Ni–Mo type catalyst was reported to even outperform Pt, which only requires an overpotential of 44 mV with the iR compensation at a current density of 200 mA cm^{-2} [9]. On the other hand, outstanding stability especially at high current density was also obtained for non-noble metal catalysts [10]. In particular, Phosphorus (P) element is found to be beneficial to the long-term stability of HER catalysts at high current density. For example, it was reported that the Co–P catalyst could persist for 3000 h at 1000 mA cm^{-2} without substantial decline in 1 M KOH [11], and the v- $Ni_{12}P_5$ endured running a 10 000 CV test between 0–500 mA cm^{-2} [12]. Other non-noble metal/nonmetal catalysts were also reported to achieve remarkable HER performance. For example, Tantalum (Ta) [13], Molybdenum (Mo) [14, 15], and Selenium (Se) [16], when combined with Sulfur (S) [17, 18], Carbon (C) [19, 20], Nitrogen (N) [21, 22] and/or other nonmetallic elements [23], could facilitate HER kinetics and exhibit prolonged lifetimes.

While although numerous catalysts were suggested as promising for efficient HER, the reported overpotentials in recent studies were mostly obtained with the iR compensation corresponding to the ohmic drop energy loss [24, 25]. The purpose of iR compensation (iR correction) of HER catalysts is to focus on the catalyst itself and get rid of the environment influence. But it is impractical or even impossible for the HER catalyst escaping from the influence of the environment, and the same catalyst could exhibit different overpotentials after iR correction when loaded on different supports [26, 27]. Even worse, sometimes the iR compensation part could make up to nearly 90% of all the input energy, in other word, the reported overpotential corresponds to only 10% of the actual consumed energy [28]. In practice, the ultimate goal is to realize large scale hydrogen production with high energy conversion efficiency (ECE) using energy-saving catalysts, while the

non-HER energy loss including the iR compensation part definitely cannot be ignored.

One possible reason for the seemingly underestimation of energy consumption in developing HER catalysts is that in many studies the energy efficiency is measured in terms of the whole water splitting process in a water electrolyzer (WE) constructed based on proton exchange membrane (PEM) or anion exchange membrane (AEM). In the configurations of PEMWE or AEMWE for water electrolysis, the equivalent series resistance is normally small ($\sim 0.1 \Omega$ or less) and therefore the corresponding energy loss is small unless for ultrahigh current density. There is no doubt that the overall water splitting in PEMWE and AEMWE cells are more realistic towards commercial applications than the single electrode reaction in standard triple electrode systems. However, the former experiments involve more control factors than the latter, and the corresponding performance optimization is more related with solving technical rather than scientific problems. We never intend to underestimate the merit of direct optimization of whole WEs such as PEM/AEM cells, but we emphasize on that the advantage of studying the single electrode reaction is that the reduction of the complex problem to fundamental processes involving minimized control factors. This is why it is more convenient and effective to develop electrocatalysts for single electrode reactions such as HER.

The performance optimization of HER electrocatalysts mainly focuses on the catalyst itself as well as necessary substrates or supporting materials. The intrinsic activity of the catalyst is determined by the reactant (and/or product) catalyst interactions augmented by the catalyst substrate interactions, for which the structure of catalyst and support play an important role. For example, it has been widely accepted that the nanostructure of HER catalysts could provide abundant active sites and facilitate the mass transfer and bubble release. And extensive studies on the substrate or support effect for HER catalysts have been done [29, 30] since practically most if not all HER catalysts must be loaded on the support, and the support effect may substantially influence the iR compensation and the overall energy efficiency. Nevertheless, the energy consumption for HER including the energy loss associated with iR compensation is rarely discussed. We want to make it clear that the support here refers to the substrate as a free-standing electrode on which the electrocatalyst can be loaded. There are a variety of supporting materials especially carbon-based supports such as carbon powder or carbon nanotube (CNT) used as an intermediate medium between the catalyst and the electrode to increase the compatibility of the two components. Although the carbon-based supporting materials could facilitate the electron transfer, provide ample active sites, and prevent the agglomeration of catalyst, which is particularly beneficial to dispersed catalysts such as single atom catalysts, they cause additional energy loss if used in combination with other electrodes such as glass carbon electrode or metal electrodes, and therefore the support induced non-HER energy loss include contributions from both carbon additives and the substrate electrode. Even some of them such

as CNT could be made self-standing as the electrode, the corresponding series resistance is normally larger than that of the electrodes made of metal foams. In contrast to the conventional protocol in which various catalysts are loaded on the same standard electrode (e.g. glass carbon electrode) and the performance of the catalyst is evaluated after the iR compensation is made, we advocate the alternative evaluation protocol in which the overall performance of the catalyst and its supporting electrode is examined, and therefore the compatibility of the catalyst and the support and the ECE of the overall catalyst/support complex are of great importance.

The energy loss associated with iR compensation is also a key factor when evaluating the long-term stability of HER catalysts. Compared with short time activity, long-term performance is usually examined at relatively large current density to mimic practical operating conditions. Under such harsh conditions, the structural influence and the support effect are expected to be more prominent. Presumably a good support requires a small compensation for the ohmic drop energy loss and the structures of both catalyst and support and their compatibility may determine how these structures and HER performance evolve during the durability test at large current density.

In this mini-review, from the view of energy consumption in the overall HER process, we summarize the influence of different supports on the iR compensation for HER catalysts. To make the discussion more organized, current HER catalyst supports are classified as metal foams, non-metallic compounds, composite materials, and other new types of materials. Remarkably, this review proposes to rate HER electrocatalysts by using an ECE for the overall water electrolysis in its single electrode reaction limit. This energy label is applied to evaluate the HER performance of electrocatalysts for both the transient activity and long-term stability. Also discussions are made on the compatibility of the catalyst and the support, the structural influence such as size and geometrical shape on the long-term stability of the catalyst, and the connection with the overall water electrolysis in PEMWE and AEMWE. Finally, the challenges and opportunities for developing practical HER electrocatalysts are discussed and proposed.

2. The support influence on the energy consumption for HER catalysts

2.1. Energy consumption and iR compensation

Ideal high performance HER electrocatalyst should drive HER at low energy consumption. The minimal driving force for HER may be expressed in terms of the standard electrode potential according to the Nernst equation, while the extra energy cost required to overcome the activation barrier, and the non-HER energy loss, is represented by the overpotential. Conventionally, the non-HER energy loss part may be subtracted from the applied potential through the iR compensation assuming a Coulomb efficiency of 100%. There are primarily two ways to manually deduct the iR compensation part. The first method is to deduct a fraction of α (85%–90%) of all the

overpotential applied for HER as given in equation (1). And the second method is to deduct part of the overpotential caused by the Joule heat loss, in terms of the nonreactive resistance as shown in equation (2),

$$E_{\text{compensated}} = E_{\text{app}} - \alpha E_{\text{app}} \quad (1)$$

$$E_{\text{compensated}} = E_{\text{app}} - \beta iR_s. \quad (2)$$

Here E_{app} is the applied overpotential for HER, and $E_{\text{compensated}}$ is the overpotential after iR compensation. R_s is the series or solution resistance (see below), i is the current and β takes a value in the range of 85%–100%. The first method simply assumes that a constant proportion of the applied overpotential can be attributed to the non-HER energy loss, but obviously the non-HER proportion may not be a constant as the current density changes. The second method seems more reasonable, but the overpotential caused by environment still accounts for a huge proportion and some uncertainties exist. Automatic iR compensation may be performed by the electrochemical workstation but involving more complex treatments such as the variation of R_s with respect to current density. In fact, the drawbacks of iR compensation during HER have already been noticed and discussed [26, 27], and the linear sweep voltammetry (LSV) curves in figures 1(a)–(e) clearly show the disparity of overpotentials obtained with or without iR compensation.

Adopting iR compensation or not, the R_s in equation (2) is definitely a good measure of the non-HER energy loss and may be related with the ECE of the catalyst. Here R_s is defined in a general sense including the series resistance of the solution as well as the whole catalytic system, i.e. the electrocatalyst itself and the support, and can be written by

$$R_s = x/KA. \quad (3)$$

For a typical three electrode system, x is the distance between the working electrode and the reference electrode, but equation (3) may become invalid when x is too small to guarantee the clearance of the charge transfer pathways. The conductivity of the HER catalyst system K is inversely proportional to R_s , and therefore efficient electron transport can promote HER dynamics. The area A corresponds to the effective surface area of the working electrode.

In fact, the microscopic morphology of the catalyst does affect R_s , and high specific surface area may reduce R_s appreciably, e.g. soaking the same sample of Ni@AABS in 6 M KOH results in Ni(OH)₂/Ni@AABS with an increased specific surface area and a lower R_s [33]. Of course, the specific surface area is not the only factor to control R_s . For example, the R_s of Ni/Mo₂C_(1:2)-NCNFs produced from electrospinning process could be as high as 5 Ω due to the used nanofiber of low conductivity [34], although the polymer materials have large specific surface area. In addition, the conductivity K may become a comprehensive parameter for complicated systems, including various contributions from the distance and position of the working electrode and counter electrode, the transport capability of the electrolyte, and even the properties of

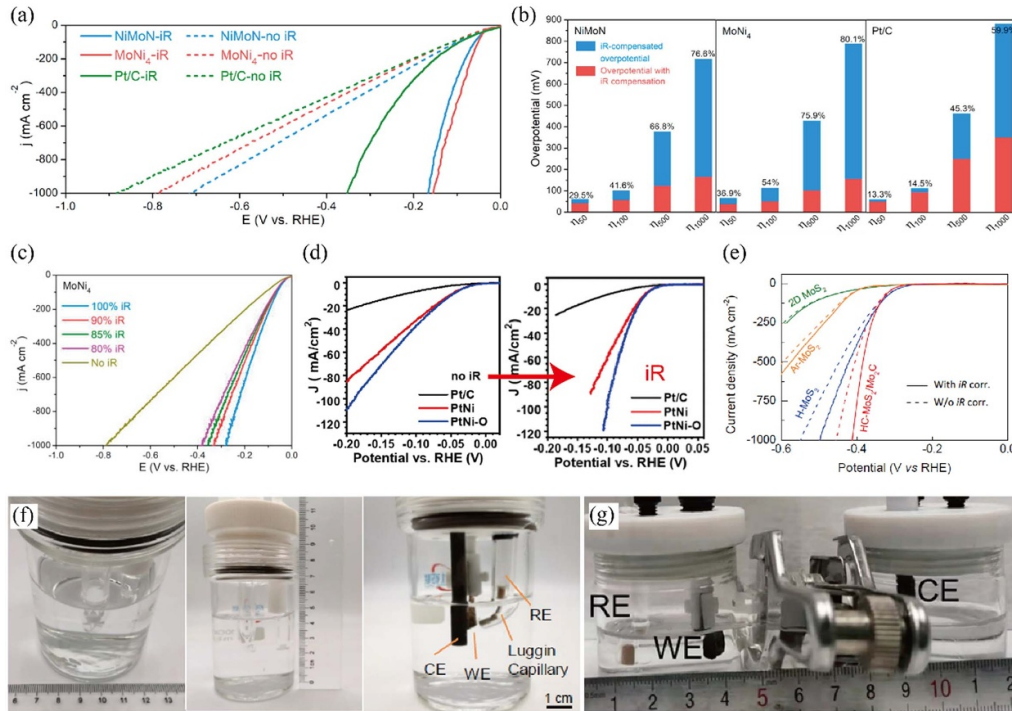


Figure 1. The effect of iR compensation and typical electrochemical cells for HER. (a) LSV for different catalysts with and without iR compensation. (b) The proportion of the iR compensation part of overpotential. (c) The effect of iR compensation for LSV using different percentages in the deduction. Reprinted from [27], © 2020 Elsevier Ltd All rights reserved. (d) LSV curves of Ni based catalysts with and without iR compensation. Reprinted with permission from [31]. Copyright (2018) American Chemical Society. (e) LSV curves of MoS₂ based catalysts; (f) The corresponding test device for HER in (e), note that the special configuration of the electrodes results in small iR compensation. Reproduced from [32]. CC BY 4.0. (g) Typical double groove cell for HER test. Reproduced with permission from [33]. CC BY-NC-ND 4.0.

the test container. Figures 1(f)–(g) display some typical HER test systems reported in the literature. Note that in the laboratory studies conventional settings are adopted with the surface area of catalyst being 1 cm² and close distances on the order of a few centimeters among working, reference, and counter electrodes.

The adoption of a universal experimental settings would allow for a meaningful comparison of ECE of electrocatalytic HER. ECE is a widely used criterion for the performance evaluation of energy transformation devices such as heat engine, solar cells, and fuel cells. In fact, for the overall water electrolysis, the ECE is well defined, i.e.

$$\begin{aligned} \text{ECE} &= \frac{\text{Required energy}}{\text{Input energy}} \times 100\% \\ &= \frac{\text{Equilibrium potential}}{\text{Applied potential}} \times 100\%. \end{aligned} \quad (4)$$

For example, if the applied potential is 1.7 V for the electrolysis at 25 °C ($E^0 = 1.23$ V), the ECE is $1.23/1.7 = 72.4\%$. Equation (4) is the ECE for a single WE cell with no technical considerations on any accessories associated with extra energy contributions such as heat bath, or reuse of waste heat etc. And it is not recommended to replace the equilibrium potential by the so-called thermal neutral voltage (1.48 V at 25 °C) or lower heating value at elevated temperatures since here we are interested only in the efficiency of water electrolysis rather

than its coupling with external energy resources such as heat bath or heat engine. However, as far as we know, there is no well-defined ECE for HER. Nevertheless, we find an upper limit of the ECE for HER to be useful for the performance evaluation [10], i.e.

$$\text{ECE}_{\text{ul}} = \frac{\text{Equilibrium potential}}{\text{Equilibrium potential} + \text{overpotential}} \times 100\%. \quad (5)$$

For example, if the applied overpotential is 100 mV for HER at 25 °C ($E^0 = 1.23$ V), the ECE_{ul} is $1.23/1.33 = 92.5\%$. Here we simply assume that the overpotential for oxygen evolution reaction (OER) is zero and all electric energy is used for HER, i.e. 100% Coulomb efficiency. Although the ECE_{ul} is only the upper limit of the HER efficiency, it is still useful in making a qualitative evaluation especially for the systematic comparison among a series of control experiments, such as screening best catalysts or optimized fabrication conditions.

To rate the performance of HER electrocatalysts straightforwardly, we propose to introduce an energy label comprising five levels based on ECE, as shown in table 1, which also lists the corresponding label for the overall water electrolysis. For example, the top level HER electrocatalyst is expected to require an overpotential no more than 140 mV, whereas the applied potential for the top level OWE is no more than 1.37 V.

Table 1. Energy label for HER and overall water electrolysis (OWE). * The potential is referred to the standard equilibrium (cell) potential at 25 °C ($E^0 = 1.23$ V).

Levels	I	II	III	IV	V
ECE (%)	[90, 100]	[80, 90]	[70, 80]	[60, 70]	[0, 60]
HER over potential (V)*	≤ 0.14	[0.14, 0.31]	[0.31, 0.53]	[0.53, 0.82]	≥ 0.82
OWE applied potential (V)*	≤ 1.37	[1.37, 1.54]	[1.54, 1.76]	[1.76, 2.05]	≥ 2.05

Table 2. HER properties of some reported catalytic systems using metal foam as support. Ni foam (NiF); copper foam (CuF); iron foam (FeF); cobalt foam (CoF).

Catalyst	Support	Electrolyte	R_s (Ω)	η : mV/100 mA cm ⁻²	ECE (%)
				With iRC	
Ni ₂ (1-x)Mo _{2x} P [35]	NiF	1 M KOH	1	162	82.4
MoP/Ni ₂ P [36]	NiF	1 M KOH	>1	191	80.9
MoS ₂ /Ni ₃ S ₂ NWNF [37]	NiF	1 M KOH	>1.5	137	81.1
MoNi ₄ [9]	NiF	1 M KOH	0.94	33	90.6
NiCo ₂ S ₄ /Ni [38]	NiF	1 M KOH	>1	>300	75.5
Ni(OH) ₂ NiMoO _x [39]	NiF	1 M KOH	1	134	84.0
NiCoP-p [40]	NiF	1 M KOH	1.54	122	81.7
MoO _x S _y /Ni ₃ S ₂ /NF [41]	NiF	0.5 M H ₂ SO ₄	2	>350	69.1
Pt/NiO@Ni/NF [42]	NiF	1 M KOH	>0.4	>60	92.5
Ni ₃ N/Ni/NF [43]	NiF	1 M KOH	>1.6	64	84.6
C-Ni _{1-x} O [44]	NiF	1 M KOH	1.6	>90	83.1
Ni/NiO@MoO _{3-x} [45]	NiF	1 M KOH	>1.5	75	84.5
MoS ₂ (1-x)Se _{2x} /NiSe ₂ [46]	NiF	0.5 M H ₂ SO ₄	2	112	79.8
SANi-I(NiO) [47]	NiF	1 M KOH	2	60	82.6
NiCo ₂ S ₄ NW/NF [48]	NiF	1 M KOH	>4	>250	65.4
v-Ni ₁₂ P ₅ [12]	NiF	1 M KOH	0.697	>75	89.5
Ni ₄ Mo/MoO _x [49]	CuF	1 M KOH	>4	115	70.5
c-Ni@a-Ni(OH) ₂ [50]	CuF	1 M KOH	>1.5	142	80.8
Ni/Cu [51]	CuF	1 M KOH	1	>150	83.1
Pt@Cu-0.3 [52]	CuF	1 M PBS	>2.5	>200	73.2
Ag@Cu ₂ O/CF [53]	CuF	1 M KOH	>1	>250	77.8
Fe@N-CNT/IF [54]	FeF	0.5 M Na ₂ SO ₄	>1	>1000	52.8
FeS@IF [55]	FeF	1 M KOH & 0.5 M NaCl	1	225	79.1
F, P-Fe ₃ O ₄ [56]	FeF	1 M KOH	>1	179.5	81.5
RuNi-Fe ₂ O ₃ /IF [57]	FeF	1 M KOH	>0.7	75	89.5
Co ₄ S ₃ @Co foam [58]	CoF	1 M KOH	>1	>250	77.8

2.2. The influence of support for iR compensation

2.2.1. Metal foam as support for HER electrocatalysts.

Metal foam is a typical HER electrocatalyst support with the combinational advantages of high specific surface area and high conductivity. The reported R_s of the prepared catalysts is around 1 Ω , as listed in table 2, although in different catalyst systems there may contain different chemical elements or microstructures. Few exceptions with a R_s greater than 2 Ω may be attributed to the low ion conductivity of the electrolyte, poor interfacial contact and therefore large interfacial resistance. Generally speaking, Ni foam is the most frequently used HER electrocatalyst support, since Ni itself shows the capacity for HER and is earth abundant. The HER active materials could be grown *in-situ* on Ni foam in a variety of friendly and simple ways, such as electrodeposition, hydrothermal, and phosphorylation. As shown in figures 2(a)–(f), the width of basic structure of these catalysts is about 60 μm despite of

different specific surface area or test installation. Although the support influence for R_s is the same, not all the Ni foam supported catalysts take the same R_s value, and the small variations may be attributed to the differences in the specific surface area and conductivity of the loaded catalyst and the interfacial resistance between the catalyst and the support.

The copper (Cu) foam is another prevailing support for HER active materials due to the low cost and high conductivity. The typical width of the basic unit of Cu foam is around 50 μm . And the reported R_s value of catalysts supported by Cu foam ranges from 1–5 Ω (figures 2(g)–(i), table 2), although the conductivity of Cu foam is higher than that of Ni Foam. Thus, it implies that the conductivity of the support is an important factor but not the only one to determine the series resistance. In fact, the HER performance is sometimes not expected to be heavily dependent on the support since HER occurs mainly on the catalyst surface. And it was reported that

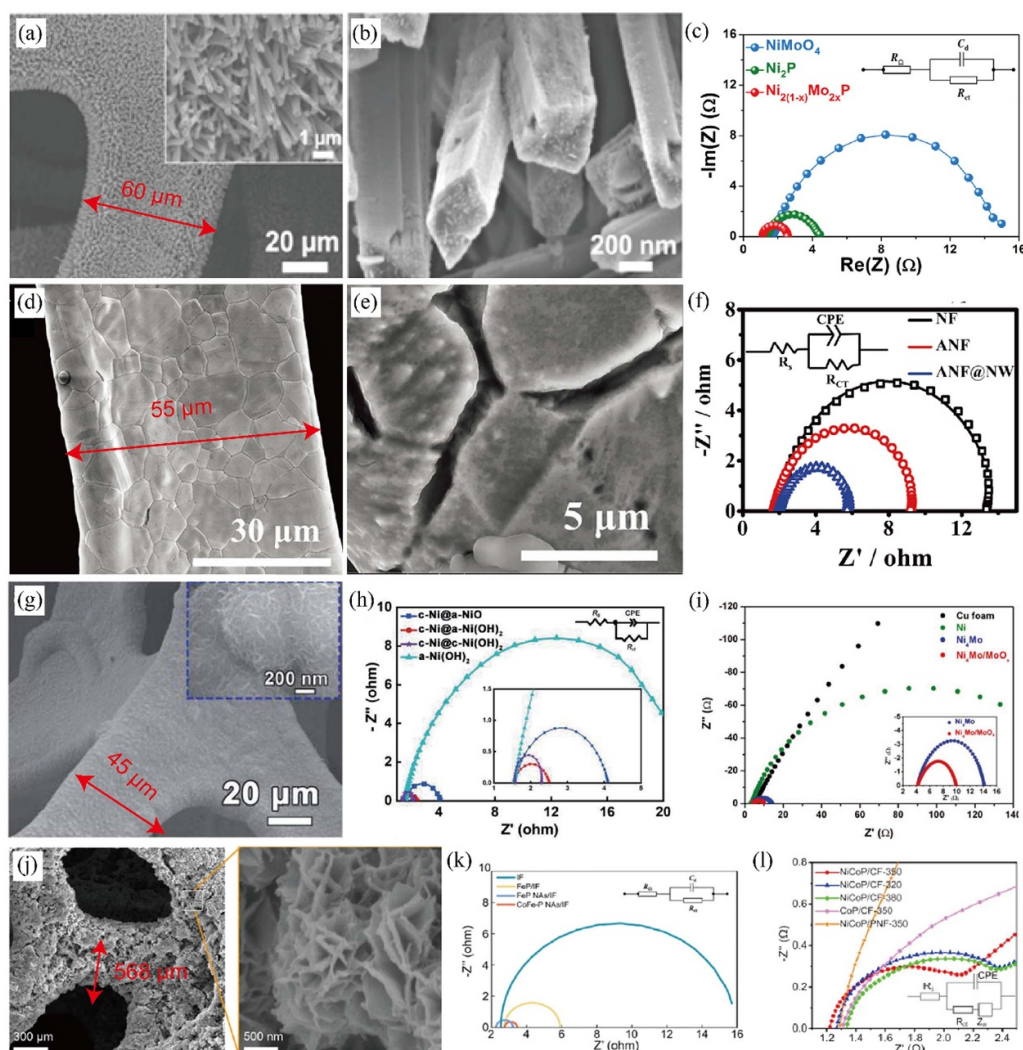


Figure 2. The morphology and EIS spectra of HER catalysts using metal foam as support. (a)–(c) SEM and EIS of Ni based catalysts using Ni foam as support. Reprinted from [35], © 2018 Elsevier Ltd All rights reserved. (d)–(f) SEM and EIS of Ni foam support [59]. John Wiley & Sons. © 2018 WILEY-VCH Verlag GmbH & Co. KGaA, Weinheim. (g)–(h) SEM and EIS of Ni based catalysts using Cu foam as support. Reproduced from [50] with permission from the Royal Society of Chemistry. (i) EIS of Ni based catalysts using Cu foam as support [49]. John Wiley & Sons. © 2019 WILEY-VCH Verlag GmbH & Co. KGaA, Weinheim. (j)–(k) SEM and EIS Fe based catalysts using Fe foam as support. Reproduced from [60] with permission from the Royal Society of Chemistry.

‘support effect’ would be effective only within the range of nanoscale from the support/catalyst interfaces. However, here we note that this ‘support effect’ is referred to the catalyst performance after making the iR compensation, while the support effect on R_s , and on the overall HER performance could be substantial. Other metal foams including iron foam [29] (figures 2(j) and (k)), silver foam [62], and Cobalt Foam [61] were also adopted as the HER catalyst support.

2.2.2. Non-metallic support for HER electrocatalysts. Non-metallic support is another important type of support for HER catalysts. This type of support has relatively low conductivity but features high specific surface area, as well as simple and friendly manufacturing procedure. The mostly-used non-metallic support is perhaps carbon cloth or fiber (CC/CF), which have higher R_s than metallic supports in general. As

shown in table 3, the R_s of CC/CF falls in the range of 1.8–7.5 Ω in our survey. The active materials loaded on CC/CF are often composed of metals, alloys, or metal compounds, which exhibit a lower conductivity than that using corresponding pure metals as support, resulting in less efficient electron transport during the HER process. As shown in figures 3(a) and (b), the basic unit of the HER catalyst supported by CC/CF is about 10 μm , and the morphology of the catalyst surface is decorated with detailed structures on the nanoscale including nanowire, nanosheets, or nanoparticles, which in this sense shows no essential difference from those loaded on metallic supports. Also small variations in R_s can be found due to different catalyst substrate interactions (see for example figure 3(c)).

Glassy carbon electrode is commonly used as the support for catalysts not being self-supported during the HER process, especially for the Pt-based catalysts. Here the self-supported

Table 3. Summary of the HER properties of reported catalytic systems using non-metallic support or other new types of supports. Yang *et al* [63] *j*: 50 mA cm⁻². Li *et al* [64] *j*: 1000 mA cm⁻².

Catalysts	Electrolyte	Support	R_s (Ω)	η : mV/100 mA cm ⁻²		ECE (%)
				With <i>i</i> RC	Without <i>i</i> RC	
n MoO ₃ /Ni–NiO [65]	1 M KOH	CF	1.8	162	/	73.6
NiMoN [66]	1 M KOH	CF	>7.5	>150	/	57.8
NiSe ₂ [67]	/	CF	2.5	>200	/	73.2
N-NiS ₂ /CF [68]	1 M KOH	CF	2.33	>200	/	74.0
S-Mo ₂ C [69]	1 M KOH 0.5 M H ₂ SO ₄ 1 M PBS	CF	3.0 2.1 6.6	>100 >50 >400	/	75.5
CoP/Ni ₂ P/CC-4 [70]	0.5 M H ₂ SO ₄	CC	>2	123	/	79.2
SIS Ni–Co [71]	/	AgNWs@CF	1	>110	/	85.5
Co@CNTs-CC [72]	1 M KOH	CNTs/CC	>2.5	>200	/	73.2
NiP ₂ –FeP ₂ [73]	/	CuNW/CuF	2	>200	/	75.5
Ir–NiMoP–NiMoPxOy/CNTs–Gr/Cu [74]	1 M KOH /	CNTs–Gr/Cu	>1.3	>250	/	76.4
MHCF–CNTs@PEMAc [63]	1 M KOH 0.5 M H ₂ SO ₄ 1 M PBS	GC	4 5 10	>300 200 >200	/	63.7
Mo ₂ C/MoC/CNT [64]	1 M KOH	CNT film	>2	233	/	74.0
MoC–Mo ₂ C–790 [75]	0.5 M H ₂ SO ₄	Mo plate	>1	190	>500	71.1
NiO/Ni(OH) ₂ /Ni@AABS [33]	1 M KOH	AgNW aerogel	0.33	/	77	94.1
Pt–Ni(N) NWs [76]	1 M KOH	GC/Nafion	6	50	>150	89.1

catalyst means that it can be made as the free-standing electrode rather than that it can be directly bound to the substrate electrode without using supporting additives. The commercial Pt/C is usually referred to be the most promising HER catalyst, and the powder Pt/C has a theoretical specific surface area higher than 950 m² g⁻¹. Unfortunately, Pt/C is not a self-supported electrode and has to be bound to other supports using a binder such as Nafion, which could significantly reduce the specific surface area and conductivity of the catalyst. As illustrated in table 3, the Pt based catalysts supported by glassy carbon electrode with the aid of Nafion have a R_s around 5 Ω , which may lead to substantial energy overhead during practical HER processes.

CNT is a newly emerging type of support for HER catalysts, which has the advantages of low cost, robust mechanical properties, and being environmentally friendly, while the corresponding production process of CNTs is still under further exploration. Not only the CNT film was used as the free-standing electrode [64], but also it was reported that when composited with N-doped carbon framework, CNT

based nanocarbon complex showed notable HER activity as a metal-free catalyst although trace metal impurities inside CNT was claimed to be inactive for HER [63]. The R_s of the CNT film electrode is larger than 2 Ω , which is higher than normal metallic supports. Rather than being used as self-standing support, CNT is also a frequently used supporting additive to enhance the compatibility between powder catalysts and traditional supports such as Ni foam [80, 81], the carbon cloth or fiber [82–84], and Glassy carbon [85, 86] etc, which offers high specific surface area, and conducive pathways connecting the loaded catalyst and the supporting electrode. However the series resistance of the catalytic complex depends on the specific structure of CNT and catalyst substrate interactions as well as the electrical conductivity of the supporting electrode. For example, the SEM images of HER catalyst supported by CNTs (figures 3(d) and (e)) indicate that the basic unite is on the nanoscale and the diameter is only about 15 nm. Although this type of HER catalyst has high specific surface area, the active materials distribution on the CNTs is not uniform (figure 3(d)), and therefore electron transport does not

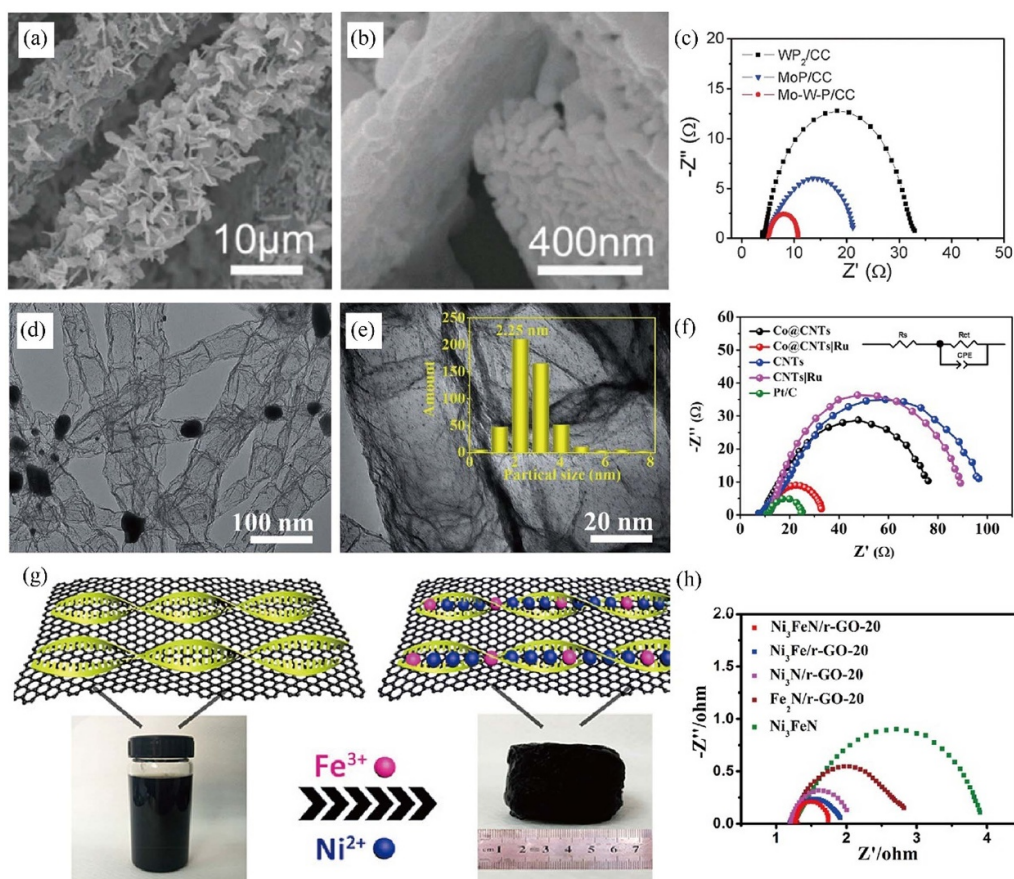


Figure 3. The morphology and EIS spectra of HER catalysts using non-metal foam as support. (a)–(c) Carbon cloth support. Reproduced from [77] with permission from the Royal Society of Chemistry. (d)–(f) Carbon nanotubes support. Reproduced from [78]. CC BY 4.0. (g) Schematic illustration of $\text{Ni}_3\text{FeN}/\text{r-GO}$ catalysts, and (h) Nyquist plots of $\text{Ni}_3\text{FeN}/\text{r-GO}$ at 200 mV. Reprinted with permission from [79]. Copyright (2018) American Chemical Society.

proceed smoothly since the CNTs themselves are not uniform either and exhibit a low conductivity. Consequently, the catalyst supported by CNTs could have a R_s as high as 10 Ω , as shown in figure 3(f). Still, the CNT supporting additive may find its wide application in PEM and AEM systems of water splitting, just like its carbon powder counterpart in Pt/C, due to the compact configuration of WEs.

Graphene oxide-based composite material is another type of supporting material for HER catalysts, which have garnered much attention due to its excellent electron transport properties in comparison with other non-metallic supports [87]. However, this category of materials is often not self-supported, thus needs to be used in combination with glassy carbon electrode and binders such as Nafion, just like Pt/C powder. Generally speaking, the R_s of the catalyst with this type of support is higher than the counterpart using metallic supports. As an example, the R_s of $\text{Mo}_2\text{C}@ \text{NPC}/\text{NPRGO}$ is higher than 5 Ω according to the EIS curves [87]. By contrast, another catalyst with graphene oxide loaded on Ni foam ($\text{Ni}_3\text{FeN}/\text{r-GO-20}$) has R_s around of 1.2 Ω according to the EIS curves (figures 3(g) and (h)). Similar to graphene oxide, MXenes are also a new type of supporting material that is not self-supported [88].

2.2.3. Other new supports for HER electrocatalysts.

Metallic-aerogels could be used as a new class of support. In particular, the free-standing silver nanowire (AgNW) aerogel-based support (AABS) has the merits of high specific surface area, high conductivity, and low density. Electrocatalysts for HER supported by AABS (figures 4(a)–(c)) exhibited a low R_s around 0.33 Ω , and two representative catalysts $\text{NiMoP}@ \text{AABS}$ and $\text{NiO}/\text{Ni}(\text{OH})_2/\text{Ni}@ \text{AABS}$ achieved an overpotential of only 87 mV and 77 mV at a current density of 100 mA cm^{-2} without iR compensation, respectively, which are much lower than most electrocatalysts reported in the literature [33]. The excellent HER performance of AABS catalysts is attributed to the nano effect induced by AABS. In comparison with the catalysts loaded on the conventional supports on the micrometer scale, as shown in figure 4(a), the basic unit of AABS is on the nanoscale, and this structure presumably provides numerous accessible active sites and enhances electron transport, which could significantly reduce non-HER energy and promote the dynamics of HER process.

Taking Pt aerogel as HER catalyst support has also been investigated. Recent work indicates that the Pt NW aerogel needs to be used with glassy carbon electrode and Nafion, and

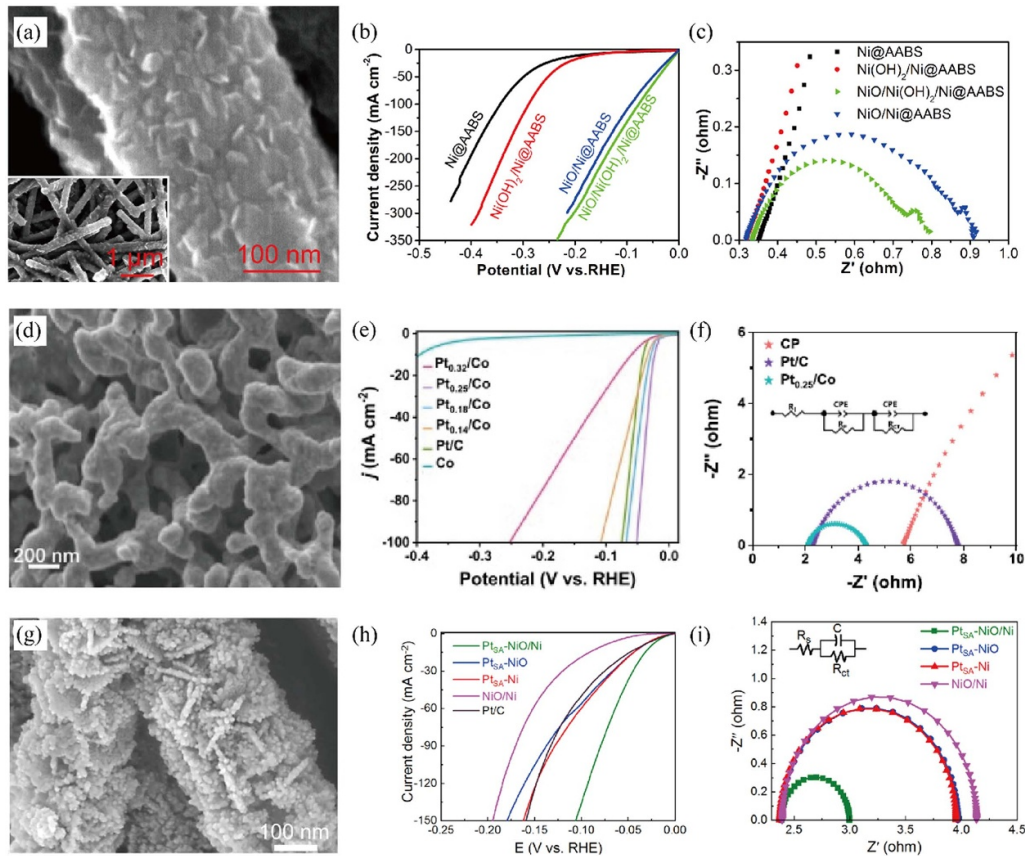


Figure 4. The morphology and EIS spectra of HER catalysts using metallic-aerogels as support. (a)–(c) SEM, LSV curves and corresponding Nyquist plots of Ni based catalysts loaded on AABS. Reproduced with permission from [33]. CC BY-NC-ND 4.0. (d)–(f) SEM image, LSV curves and corresponding Nyquist plots of Pt_{0.25}/Co on Co aerogel support. Reprinted from [89], © 2023 Elsevier B.V. All rights reserved. (g) SEM image, LSV curves and corresponding Nyquist plots of Pt_{SA}-NiO/Ni on Ag NWs. Reproduced from [90]. CC BY 4.0.

the overpotential recorded was less than 70 mV at the current density of 20 mA cm⁻² without iR compensation [91]. In order to take advantage of high specific surface area and conductivity, many HER catalysts made of metal nanowires were loaded on cloth fabric, and remarkable HER performance could be achieved. For example, Pt cluster supported Co aerogel catalyst (Pt_{0.25}/Co) obtained an overpotential of 51 mV at 100 mA cm⁻² (figures 4(d)–(f)), the Pt_{SA}-NiO/Ni exhibited an overpotential of 85 mV at a current density of 100 mA cm⁻² (figures 4(g)–(i)), and the SIS Ni-Co@Ag NWs required an overpotential around 170 mV at 300 mA cm⁻², all with 95% iR compensation [71]. The corresponding R_s were reported to be around 2 Ω for the former two catalysts and 1 Ω for the last catalyst. The large R_s values might be related with the observation that nano structures only exist on the surface of the catalyst, but the basic untie structure beneath the surface is still on the micrometer scale.

It is therefore important to note that the compatibility between the catalyst and the substrate is the key factor to control the R_s , the support effect, and even the overall HER performance. Specifically, the incompatibility between the nanostructure of catalysts and the main framework of conventional supports on the micrometer scale may lead to poor contact between the catalyst and substrate, and therefore large

interfacial resistance, which results in extra energy consumption and degraded HER performance. According to the ECE in tables 2 and 3 for representative HER catalysts, and the energy label in table 1, the catalysts loaded on metal foams are on the level II or higher, significantly better than those loaded on nonmetallic supports. This observation indicates that the high conductivity of the support also helps to reduce the non-HER energy loss.

3. Long-term stability of HER catalysts: structural influence and energy efficiency

The long-term stability of HER catalysts is one of challenging bottlenecks for practical applications. In this section, the structural influence including morphology, size, and dimensions on the long-term stability of HER catalysts will be addressed first. Particle, wires, sheets, or column are the commonly observed structures for the HER electrocatalysts, and the fundamental differences among different catalysts are the size and density. These structural differences may have an impact on various aspects including electronic transmission, the desorption and adsorption of H₂, and the role of force during the HER process, which will eventually have an influence on the long-term

Table 4. Summary of the stability properties of reported catalysts.

Catalysts	η : mV ($j = 1 \text{ A cm}^{-2}$)		Time (h) ($j = 1 \text{ A cm}^{-2}$)	ECE (%)
	With <i>i</i> RC	Without <i>i</i> RC		
Mo ₂ C/MoC/CNT [64]	233	>700	336	63.7
Mo-NiP@NF [93]	282	$R_s > 1.8$	1500	37.1
W _{0.05} -RuP ₂ @C ₃ N ₄ -NC [94]	194	/	400 (0.5 A) 600 (1 A)	
Ni-chip [95]	297 mV	/	1070 h	
MoS ₂ /Ni ₃ S ₂ NW-NF [37]	200	>850	12	59.1
NiP ₂ -FeP ₂ -CuNW/CuF [73]	>350	$R_s > 2$	50	34.4
Ni ₂ P-Ni ₅ P ₄ @AABS [10]	/	687	1008 (0.5–1 A)	64.2
Ni _{0.95} Cu _{0.05} DSS [96]	426	$R_s > 2.5$	110	42.0
Pt SAs/MoO ₂ [97]	>600	$R_s > 5$	200	18.0
Ni ₂ P-Fe ₂ P [98]	389	$R_s > 2$	23 (0.5 A)	34.0
Ni ₃ Mo ₃ N [99]	>700	$R_s = 2.66$	50 (1.1 A)	27.0
WC-N/W [100]	>400	$R_s > 1$	>20	46.8
P-Fe ₃ O ₄ /IF [101]	>220	$R_s > 1$	20 (0.5 A)	50.2
P-NiMoHZ [102]	210	/	200	
α -MoB ₂ [103]	334	$R_s > 5$	60 (3.6 A)	18.7
NiCoP [104]	295	$R_s > 1.6$	25	39.4
3F-FeP [105]	302	>2300	24	34.8
A-NiCo LDH/NF [106]	381	$R_s > 2$	72	34.1
F-Co ₂ P/Fe ₂ P/IF [107]	260.5	/	10	
Co/Se-MoS ₂ -NF [108]	382	>1350	360	47.7
NiFe ₂ O ₄ [109]	>1500	$R_s > 2$	60	26.0
CoFeOH/CoFeP/IF [110]	221.8	>1500	100	45.1
Ru-Mo ₂ C@CNT [111]	78	$R_s > 2$	1000 (0.5 A)	37.2
Ru-1.0 [112]	>200	$R_s > 7.5$	100	13.8
R-CoC ₂ O ₄ @MXene [113]	216	$R_s > 1$	100	50.3
V-FeP [114]	290	>1200	24	50.6
Co-Mo ₅ N ₆ [115]	280	$R_s > 2$	10	34.8

stability of HER catalysts. On the other hand, the long-term energy efficiency of HER catalysts is also discussed.

One of the most prevailing criteria on the stability of HER catalysts is to investigate the performance in a long duration at a large current density such as 1000 mA cm⁻², to match the demands in industrial applications. Here table 4 summarizes the stability performance of the state-of-the-art HER catalysts. In our survey, the porous Co-P is the most durable HER catalyst reported [11]. As shown in figures 5(a)–(d), the porous Co-P exhibited an overpotential of 290 mV at the current density of 1000 mA cm⁻² with iR compensation ($R_s \sim 0.6 \Omega$), and sustained for 3000 h with negligible degradation. The overall framework of this catalyst is the Co-P chemical compound loaded on the Co foam, and SEM images in figure 5(a) show that Co-P presents a particle-like shape uniformly covered the surface of the catalyst, and the diameter of the particles is around 100 nm. The catalyst of Co/Se-MoS₂-NF passed a stability test of 360 h at 1000 mA cm⁻², detailed in figures 5(e)–(h). Figure 5(g) displays the LSV curves of Co/Se-MoS₂-NF obtained with iR or without iR compensation, which sufficiently demonstrated the significance of iR part. SEM images in figures 5(e) and (f) show the morphology of the catalyst, indicating that the basic unit of Co/Se-MoS₂-NF is ball-like hole with the diameter of about 200 nm due to the SiO₂ template. Another typical structure is Pt/MoO₂ NRs, which maintained the stability for 200 h at 1000 mA cm⁻²,

as shown in figure 5(h), and the basic unit is the nanorod with a diameter of about 200 nm. Also UP-RuNi_{SAs}/C exhibited a good stability for 100 h at 3000 mA cm⁻², and the microscopic morphology presented a bag-like structure with a diameter of about 200 nm (figures 5(i)–(k)). Above all, the catalyst with excellent stability during the HER process seems to have a relatively large basic unit, which may be helpful to prevent the catalyst from corrosion at large current density. Consistently, a catalyst for OER, i.e. 3D-O₂-Cat-1 showed an excellent stability retaining over 6000 h at 1000 mA cm⁻² without decay [92]. The SEM image revealed that the surface of the catalyst presented a high-density lattice, and each single sheet is about 200 nm high and 200 nm wide, which is presumably robust enough for passing the large OER current density.

By contrast, the long-term stability of HER catalysts with dominated nanostructures are usually not satisfactory, although nano structures and nano interfaces are believed to be beneficial for HER dynamics, and the nano catalysts often present a nearly zero onset overpotential during HER. For example, the nano interface catalyst of Pt₃Ni₁ NWs-S/C only preserved for 5 h at 5 mA cm⁻² without iR compensation, and the basic unit of this catalyst is a nanowire with a diameter of about 20 nm (figures 5(l)–(m)).

Of course, if the nano-structure is not the only component but grows on a higher-level main structure on the large scale of micron level, the long-term stability of the catalyst could

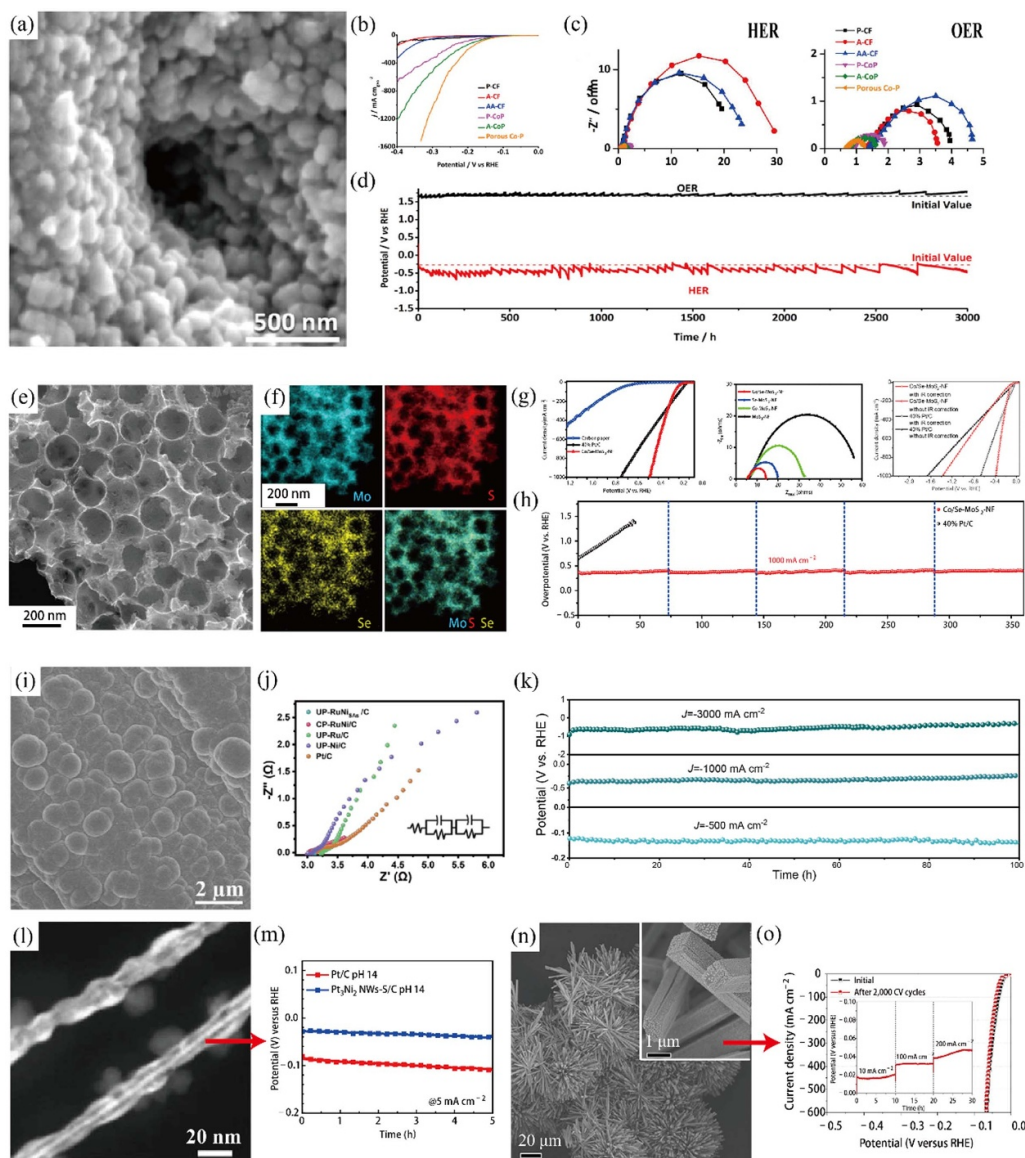


Figure 5. The morphology and HER performance of HER catalysts. Porous Co–P catalyst: (a) SEM image, (b) LSV and (c) Nyquist plots for HER and OER. (d) Chronopotentiometric curves of porous Co–P for HER at a current density of 1000 mA cm^{-2} in 1.0 M KOH . Reprinted with permission from [11]. Copyright (2020) American Chemical Society. Co/Se–Mo–S₂–NF: (e) SEM image and (f) corresponding EDX mappings. (g) LSV with or without iR compensation and Nyquist plots. (h) The chronopotentiometric curves of long-term stability for Co/Se–Mo–S₂–NF at 1000 mA cm^{-2} . Reproduced from [108]. CC BY 4.0. UP–RuNi₄S₄/C: (i) SEM image, (j) Nyquist plots and (k) long-term stability curves of UP–RuNi₄S₄/C. Reproduced from [116]. CC BY 4.0. (l) SEM image and (m) long-term stability curves of Pt₃Ni₁ NWs–S/C. Reproduced from [117]. CC BY 4.0. (n) SEM image and (o) long-term stability curves of MoNi₄. Reproduced from [9]. CC BY 4.0.

be improved. For example, Cu NDs/Ni₃S₂ NTs hold an HER stability for 30 h at the current density of around 90 mA cm^{-2} , the basic unit of which is the high density nanointerfaces on the wires with the diameter of about $2 \mu\text{m}$ [118]. Above all, the long-term stability of HER catalysts seems to favor the characteristic microstructure at micron level, and a relatively simple chemical composition. Just like the old Chinese saying goes, Greatness in Simplicity.

On the other hand, nanosizing the catalyst and/or the support may introduce numerous active sites and therefore increase the HER activity. Thus, how to reconcile high activity

and low stability is worthwhile investigating for future studies. Also constructing an integrated framework incorporating compatible catalyst and substrate is crucial to achieve optimal overall HER performance.

In comparison with tables 2 and 3, the ECE of representative HER electrocatalysts during long term tests are significantly lower (table 4), which is due to the substantially increased current density (from 100 mA cm^{-2} to 1 A cm^{-2}) and the non-HER energy loss. In fact, most catalysts in table 4 are on the lowest level according to the energy label proposed in table 1. This suggests that plenty of room is available for

further improvements on the durability of HER electrocatalysts under large current density. Again, the catalyst substrate interactions and compatibility are important in searching better catalytic systems with high ECE.

4. PEM and AEM systems

For the mass production of H₂, the alkaline WE (AWE) as shown in figure 6(a) has been put in industrial applications for many years. While the disadvantages of AWM include the safety issues due to the easily mixing of the products H₂ and O₂, and low current density indicating the low efficiency of the system. As the promising candidates for the next generation WE, the cells built based on solid polymer of PEM or AEM (figures 6(b) and (c)) receive predominant attentions in recent years, which may compensate the drawbacks of the AWE system. In particular, the AEMWE system is even close to be industrialized, which could completely dispense with precious metals such as platinum (Pt), iridium (Ir) and Ruthenium (Ru).

Whichever AWE, PEMWE or AEMWE is used, the fundamental HER process is the same to that occurs in the two-electrode or three-electrode systems in laboratory, and the major difference is that the former setups focus more on cost control and involve more technical problems including operating at high temperature (say 50 °C–90 °C), high pressure and with flowing electrolyte etc. The demands for the high-performance catalyst in PEMWE or AEMWE systems are similar to that for AWE, but with more stringent requirements on the structure stability due to high operating temperature and pressure. The energy loss corresponding to the *iR* drop part does not seem to take a significant portion due to the ultrashort distance between cathode and anode, but *R_s* inevitably exists and even changes with the temperature or current density of the cell system, which leads to the reduction of electrolytic efficiency [120]. As shown in figure 6(d), the *iR* compensation part is about 0.1 V at 1.0 A cm⁻² of the AEMWE cell. Note that here *R_s* is the series resistance of the whole system including contributions from both HER and OER catalysts, and depends on various factors including electrical conductivity, specific surface area, support of the catalyst, and other parts of the WE cell.

For the PEMWE system, the Pt based HER catalysts are often used in couple with Iridium based OER catalysts to achieve gratifying performance in the acidic environment. The loading mass of Pt is often around 0.5 mg cm⁻², and excellent long-term stability can be observed at large current density around 1 A cm⁻². However, the applied potential is about 1.7 V or more in most cases, which corresponds to an ECE of 72% or less for a single PEMWE cell. In addition, as shown in the figure 6(e), the PEM may be contaminated during the long-term operation, which leads to decreased efficiency, reduced cell lifetime and safety issues. The non-noble metal catalysts have also been extensively investigated. For example,

the Cobalt based HER catalyst with a belt-shaped basic unit on the micrometer level achieved a Pt-like performance with a long-term stability more than 400 h at 1 A cm⁻², as shown in figures 6(f) and (g). And a performance list of a representative collection of HER catalysts used in PEMWE and AEMWE systems can be found in table 5.

For the AEMWE systems, two central issues in the catalyst development are the search for high performance noble-metal-free catalysts and the long-term stability under large current density. For example, recent studies reported that the nickel-iron-based electrocatalyst CAPist-L1 sustained for 15 200 h at 1 A cm⁻² in 1 M KOH as OER catalyst, based on which a AEMWE cell was constructed coupled with Ni₄Mo/MoO₂ as cathode [136] achieving high current density of 7.35 A cm⁻² at 2 V with good durability of 1500 h at 1 A cm⁻². Although the OER catalyst on the anode is often taken as the more important factor due to the sluggish 4 *e*⁻ reaction kinetics, the HER catalyst on the cathode is also vital. For instance, when the HER catalyst is substituted from RuP₂ to WS₂ superstructure in AEMWE with the same anode catalyst, the applied potential at 1 A cm⁻² is decreased from 1.86 to 1.7 V [133], which corresponds to an increase of the ECE from 65% to 71%.

In both PEMWE and AEMWE, the catalyst may be loaded on either the porous transport layer (PTL) or membrane, which forms the catalyst coated substrate or catalyst coated membrane (CCM), respectively. Therefore, the property of the PTL and membrane are crucial since they also serve as the support as that in the traditional three electrode system. For example, the AEMWE cell constructed using NA-Ru₃Ni/C as both the cathode and anode catalysts exhibited a very good long-term stability of 2000 h at 1 A cm⁻². However, the incompatibility of catalyst and support leads to large *R_s* and non-HER energy loss. The applied potential is 2.05 V at 1 A cm⁻², corresponding to an ECE of only 59%, although the overpotential with the *iR* compensation is low, i.e. 53 mV@100 mA cm⁻² (figures 5(h) and (i)) [123]. By contrast, in forming CCM with PEM such as Nafion, a hot-press process may be used to ensure the catalyst such as Pt based particle completely wrapped into the Nafion, which could help improve the compatibility of catalyst and support and therefore reduce the non-HER energy loss. Due to the compact configuration of PEMWE/AEMWE cells, both catalyst substrate interaction and catalyst membrane interaction are important, and the performance optimization requires comprehensive considerations involving more factors. For example, Zheng *et al* reported [142] an efficient AEMWE with judicious choices of Ni-Fe based catalyst coupled with Pt/C, AEM, ionomer and PTL, demonstrating a good stability of 800 h at 10 A cm⁻².

Comparing the ECE for overall water electrolysis in table 5 and that for HER in table 4 at large current density of 1 A cm⁻², it is clear that the energy efficient design of WE in the cases of PEMWE and AEMWE indeed improves the long-term ECE for large scale hydrogen production. Still the state of the art OWE is on the third level according to the energy label proposed in table 1. Further investigations are required.

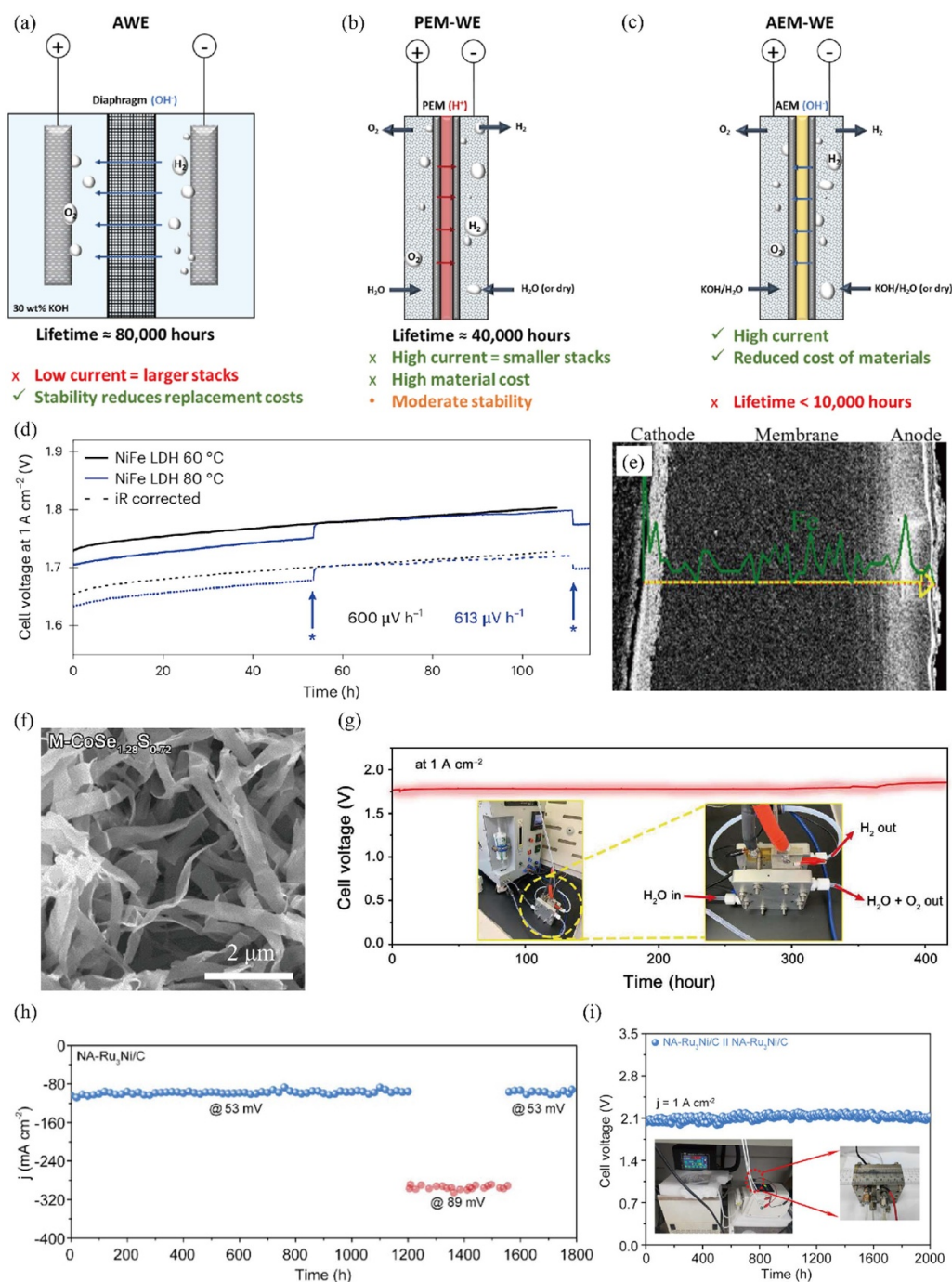


Figure 6. (a)–(c) Different industrial water electrolysis hydrogen production systems and their respective advantages and disadvantages. Reprinted with permission from [119]. Copyright (2023) American Chemical Society. (d) The effect of iR compensation for an example of the AEM system. Reproduced from [120], with permission from Springer Nature. (e) Evidence of Fe ion contamination in the PEM system, Reprinted from [121], © 2019 Elsevier B.V. All rights reserved. (f)–(g) SEM of M-CoSe_{1.28}S_{0.72} and the corresponding cell for long-term testing in the PEM system. Reproduced with permission from [122]. Copyright © 2023 The Authors, some rights reserved; exclusive licensee American Association for the Advancement of Science. No claim to original U.S. Government Works. Distributed under a Creative Commons Attribution NonCommercial License 4.0 (CC BY-NC). (h)–(i) Long-term testing of the same HER catalyst in a three-electrode system and an AEM cell, respectively, Reproduced from [123] with permission from the Royal Society of Chemistry.

5. Conclusion

The energy consumption and the associated ECE are central issues in the development of high performance electrocatalysts for HER and the overall water electrolysis. In this work,

a universal energy label comprising five levels for HER electrocatalysts is proposed based on ECE in the single electrode reaction limit, which allows for a comprehensive performance evaluation of HER electrocatalysts from the energy consumption perspective. Practically, HER electrocatalysts are

Table 5. Performance of representative HER catalysts in PEM and AEM systems.

Catalysts (PEM)		$T(^{\circ}\text{C})$	$\eta: \text{V}$	Time (h) ($j: 1 \text{ A cm}^{-2}$)	ECE ^a (%)
HER	OER				
M-CoSe _{1.28} S _{0.72} [122]	IrO ₂	60	1.79	410	68.7
Alloyed Pt SA [124]	IrO ₂	80	1.82	1000	67.6
Co ₅₉ Cu ₄₁ [125]	IrO ₂	90	1.96	48	62.8
RuP [126]	Ir	80	1.70	60 (2 A)	72.4
Cu _{44.4} Ni ₄₆ Mo _{9.6} [127]	IrO ₂	90	1.79	48	68.7
Co ₃ O ₄ [128]	IrO ₂	80	2.4	24 (1.5 A cm ⁻²)	51.3
CoP [129]	IrO _x	55	2.3	1763(1.86 A)	53.5
Pt/C [130]	IrO ₂ @TaB2	80	1.67	6000	73.7
PANI/Ni ₂ P [131]	IrO ₂	80	1.82	320	67.5
WMoC [132]	IrO ₂	80	1.89	700	65.8
Catalysts (AEM)		$T(^{\circ}\text{C})$	$\eta: \text{V}$	Time (h) ($j: 1 \text{ A cm}^{-2}$)	ECE (%)
HER	OER				
WS ₂ superstructure [133]	Commercial IrO ₂	60	1.70	1000	72.4
Ni-S-NiFe(OH) ₂ [134]	Ni-S-NiFe(OH) ₂	25	1.88	140	65.4
CoN/VN@NF [135]	P-CoVO@NF	70	1.76	1000(0.5 A)	69.9
Ni ₄ Mo/MoO ₂ [136]	CAPist-L1	80	~1.6	1500	76.9
NA-Ru ₃ Ni/C [123]	NA-Ru ₃ Ni/C	60	2.05	2000	60.0
Ni ₃ S ₂ /Cr ₂ S ₃ @NF [137]	NiFeCr LDH@NF	60	2.04	>35	60.3
VCoP-2/Ni [138]	VCoP-2/Ni	60	1.70	600	72.4
NiCoP@NiFeP [139]	NiCoP@Ni FeP	25	1.93	100	63.7
Ru SAs/WCx [140]	NiFeOH _x -NF	80	1.79	190	68.7
RuP ₂ [141]	IrO ₂	50	1.88 (0.5 A)	100 (0.5 A)	65.4

^a ECE calculated here is based on the standard equilibrium (cell) potential of 1.23 V at 25 °C.

loaded on supporting electrodes, and extra energy consumption is required for the series resistance or the corresponding iR compensation. Here the support effect on the non-HER energy loss associated with iR compensation is reviewed from the structural point of view, with the emphasis on the transient activity and the long-term stability especially under the ampere-per-square-meter-level current density. In general, nonmetallic supports of low conductivity exhibit larger R_s than metallic supports, resulting in more non-HER energy loss. The new emerging nanostructure supports could offer more accessible active sites and facile charge transport pathways than conventional micron level supports, and therefore enhance HER performance. Since supporting materials are usually more stable than the loading active materials, the long-term stability of HER catalysts seems to depend more sensitively on the active materials. Our survey on the existing literature indicates that the characteristic microstructure at the (sub)micron level, and a relatively simple chemical composition are favorable for a good HER stability. Too small in the size of nanostructure of HER catalysts may result in severe stability degradation although high activity can be achieved. Notably, the incompatibility between micron level supports and nanoscale catalysts can lead to a high R_s , and therefore cause a large amount of non-HER energy loss. The non-HER energy loss may be reduced by a variety of energy-saving designs such as shortening the distance between the cathode and anode as done in PEMWE and AEMWE for the overall water electrolysis. Nevertheless, the compact cell design and harsh operating conditions for PEMWE and AEMWE usually

introduce more involved technical issues in the energy conversion process and may require additional energy compensation from external sources, which renders the single electrode reaction such as HER an excellent testbed due to its nature of a simplified fundamental process. This work highlights the importance of the energy consumption in the global design of HER electrocatalytic systems, and the better understanding of catalyst support interactions in the further development of high-performance energy-saving electrocatalysts.

6. Future perspective

Upgrading the energy label of HER electrocatalysts in particular for the long-term performance under large current density will be challenging in future studies. Considering that fact that most current catalysts exhibit quite low ECE for HER and even for the overall water electrolysis, it seems that the rational design based on better understanding of underlying molecular mechanisms is preferred to increase the success rate. As more new catalysts have been developed, structural engineering of materials on the nanoscale is widely applied. Therefore, molecular information on the structure-property relationship would be predominant in understanding the underlying mechanism of HER. Experimental studies, in combined with theoretical modeling and computation, on either structure or dynamics, in particular on the molecular scale, could provide irreplaceable insights into the design of high-performance energy-saving HER catalysts. There are numerous interesting

topics worthwhile for future investigations, and below we suggest a few directions as examples:

- (i) The energy-saving design of the HER cell would benefit the overall electrocatalytic performance. Key cell components such as electrode and electrolyte should be optimized to further reduce the energy consumption. For example, the positioning, geometry, and the surface properties of electrodes require refined modeling and characterization. As demonstrated by the advantages and disadvantages of PEMWE and AEMWE, the global design of the electrocatalytic system in the same integrated framework with high ECE should be given more careful consideration. In particular, the compatibility of key cell components on the cell scale and the energy management of the overall HER cell are pivotal in future studies.
- (ii) More attentions should be paid on the compatibility of catalyst and support in the rational design of high-performance energy-saving HER electrocatalysts. Recent studies have already demonstrated that introducing nanostructures to catalysts or supporting materials or both may enhance HER performance. However, universal laws such as general rules that govern the structure-property-performance relationship are lacking. In addition, as the size of the basic structural unit of the support (as free-standing electrode) decreases down to the nanoscale, the characteristic size of loading active materials becomes on the same scale as that of the support, therefore the support effect may go beyond the conventional scope, for example, to synergistically couple with the interface effect, and perhaps to influence the stability. Systematical investigations on the catalyst and support interactions on the microscopic scale and their roles in reducing the energy consumption in the electrocatalytic reactions, from both experimental and theoretical perspectives, are highly valuable in uncovering the underlying mechanisms and fundamental rules of high performance HER.
- (iii) Generalizing the findings for the HER process to OER and even the overall water electrolysis deserves serious investigations in future. The underlying mechanisms may be extended beyond the HER electrocatalysts. For example, whether similar trends in the structural influence on the catalytic HER performance can be found for OER catalysts? Bifunctional catalysts that work well for both HER and OER have long been known, and the question remains unclear that whether they can achieve the best overall energy efficiency or a compatible but different HER and OER catalyst couple would be a better choice. The most difference between HER and OER is perhaps the electron transfer pathway, therefore whether and how electron transfer would affect the activity, the long-term stability of the catalyst, and the energy consumption? Investigations on such fundamental problems may require sophisticated experimental tools such as *in-situ* and operando techniques that can capture the unambiguous molecular events, as well as advanced theoretical methods/simulation packages that could treat complicated materials systems accurately and efficiently.

These examples clearly illustrate that the electrocatalytic HER is indeed a multifaceted problem with detailed structures and mechanisms on multiple scales. And a bright future of this interdisciplinary field will come under the joint efforts from researchers with different backgrounds in the continuously growing community.

Acknowledgment

We gratefully acknowledge the support from the National Science Foundation of China (51471005, 51971080).

Conflict of interest

The authors declare that they have no conflict of interest.

ORCID iD

Meisheng Han  <https://orcid.org/0000-0001-9462-3572>

References

- [1] Tonelli D, Rosa L, Gabrielli P, Caldeira K, Parente A and Contino F 2023 Global land and water limits to electrolytic hydrogen production using wind and solar resources *Nat. Commun.* **14** 5532
- [2] Xu J *et al* 2022 Frenkel-defected monolayer MoS₂ catalysts for efficient hydrogen evolution *Nat. Commun.* **13** 2193
- [3] Liu T *et al* 2024 *In-situ* direct seawater electrolysis using floating platform in ocean with uncontrollable wave motion *Nat. Commun.* **15** 5305
- [4] Liu X *et al* 2024 Enhanced HER efficiency of monolayer MoS₂ via S vacancies and Nano-Cones array induced strain engineering *Small* **20** 2307293
- [5] Zou X and Zhang Y 2015 Noble metal-free hydrogen evolution catalysts for water splitting *Chem. Soc. Rev.* **44** 5148–80
- [6] Zhou H, Yu F, Liu Y, Sun J, Zhu Z, He R, Bao J, Goddard W A, Chen S and Ren Z 2017 Outstanding hydrogen evolution reaction catalyzed by porous nickel diselenide electrocatalysts *Energy Environ. Sci.* **10** 1487–92
- [7] Luo Y, Zhang Z, Yang F, Li J, Liu Z, Ren W, Zhang S and Liu B 2021 Stabilized hydroxide-mediated nickel-based electrocatalysts for high-current-density hydrogen evolution in alkaline media *Energy Environ. Sci.* **14** 4610–9
- [8] Huo L, Jin C, Jiang K, Bao Q, Hu Z and Chu J 2022 Applications of nickel-based electrocatalysts for hydrogen evolution reaction *Adv. Energy Sustain. Res.* **3** 2100189
- [9] Zhang J, Wang T, Liu P, Liao Z, Liu S, Zhuang X, Chen M, Zschech E and Feng X 2017 Efficient hydrogen production on MoNi₄ electrocatalysts with fast water dissociation kinetics *Nat. Commun.* **8** 15437
- [10] Zuo C, Tao G, Zhong L, Zhang G, Liu B and Qiu Y 2024 Silver nanowire aerogel support promotes stable hydrogen evolution reaction at high current density *ACS Appl. Mater. Interfaces* **16** 57091–8
- [11] Li Y, Wei B, Yu Z, Bondarchuk O, Araujo A, Amorim I, Zhang N, Xu J, Neves I C and Liu L 2020 Bifunctional porous cobalt phosphide foam for high-current-density alkaline water electrolysis with 4000-h long stability *ACS Sustain. Chem. Eng.* **8** 10193–200

- [12] Duan J, Chen S, Ortíz-Ledón C A, Jaroniec M and Qiao S-Z 2020 Phosphorus vacancies that boost electrocatalytic hydrogen evolution by two orders of magnitude *Angew. Chem., Int. Ed.* **59** 8181–6
- [13] Yu Q *et al* 2021 A Ta-TaS₂ monolith catalyst with robust and metallic interface for superior hydrogen evolution *Nat. Commun.* **12** 6051
- [14] Liu H, Li X, Chen L, Zhu X, Dong P, Chee M O L, Ye M, Guo Y and Shen J 2022 Monolithic Ni-Mo-B bifunctional electrode for large current water splitting *Adv. Funct. Mater.* **32** 2107308
- [15] Liu X *et al* 2022 Activating the electrocatalysis of MoS₂ basal plane for hydrogen evolution via atomic defect configurations *Small* **18** 2200601
- [16] Yang Y, Zhang W, Xiao Y, Shi Z, Cao X, Tang Y and Gao Q 2019 CoNiSe₂ heteronanorods decorated with layered-double-hydroxides for efficient hydrogen evolution *Appl. Catal. B* **242** 132–9
- [17] Sun J, Hu X, Huang Z, Huang T, Wang X, Guo H, Dai F and Sun D 2020 Atomically thin defect-rich Ni-Se-S hybrid nanosheets as hydrogen evolution reaction electrocatalysts *Nano Res.* **13** 2056–62
- [18] Santiago A R P *et al* 2020 Tailoring the interfacial interactions of van der waals 1T-MoS₂/C₆₀ heterostructures for high-performance hydrogen evolution reaction electrocatalysis *J. Am. Chem. Soc.* **142** 17923–7
- [19] Yan B, Liu D, Feng X, Shao M and Zhang Y 2020 Ru species supported on MOF-derived N-doped TiO₂/C hybrids as efficient electrocatalytic/photocatalytic hydrogen evolution reaction catalysts *Adv. Funct. Mater.* **30** 2003007
- [20] Jia L, Liu B, Zhao Y, Chen W, Mou D, Fu J, Wang Y, Xin W and Zhao L 2020 Structure design of MoS₂@Mo₂C on nitrogen-doped carbon for enhanced alkaline hydrogen evolution reaction *J. Mater. Sci.* **55** 16197–210
- [21] Tu K *et al* 2020 A novel heterostructure based on RuMo nanoalloys and N-doped carbon as an efficient electrocatalyst for the hydrogen evolution reaction *Adv. Mater.* **32** 2005433
- [22] Qu K, Zheng Y, Zhang X, Davey K, Dai S and Qiao S Z 2017 Promotion of electrocatalytic hydrogen evolution reaction on nitrogen-doped carbon nanosheets with secondary Heteroatoms *ACS Nano* **11** 7293–300
- [23] Wang J, Liao T, Wei Z, Sun J, Guo J and Sun Z 2021 Heteroatom-doping of non-noble metal-based catalysts for electrocatalytic hydrogen evolution: an electronic structure tuning strategy *Small Methods* **5** 2000988
- [24] Ding X *et al* 2024 Dynamic restructuring of nickel sulfides for electrocatalytic hydrogen evolution reaction *Nat. Commun.* **15** 5336
- [25] Hong Y *et al* 2024 Ru₂P/Ir₂P heterostructure promotes hydrogen spillover for efficient alkaline hydrogen evolution reaction *Adv. Energy Mater.* **14** 5336
- [26] Anantharaj S, Ede S R, Karthick K, Sankar S S, Sangeetha K, Karthik P E and Kundu S 2018 Precision and correctness in the evaluation of electrocatalytic water splitting: revisiting activity parameters with a critical assessment *Energy Environ. Sci.* **11** 744–71
- [27] Yu L and Ren Z 2020 Systematic study of the influence of iR compensation on water electrolysis *Mater. Today Phys.* **14** 100253
- [28] Chen J, Xie Z, Tang Y, Tang Z and Wang X 2024 Co@Ir Core-shell nanochain aerogels for hydrogen evolution reaction and oxygen evolution reaction in alkaline media *New J. Chem.* **48** 13950–6
- [29] Zhang J, Zhang Q and Feng X 2019 Support and interface effects in water-splitting electrocatalysts *Adv. Mater.* **31** 13950–6
- [30] Zhu Y P, Guo C, Zheng Y and Qiao S-Z 2017 Surface and interface engineering of noble-metal-free electrocatalysts for efficient energy conversion processes *Acc. Chem. Res.* **50** 915–23
- [31] Zhao Z, Liu H, Gao W, Xue W, Liu Z, Huang J, Pan X and Huang Y 2018 Surface-engineered PtNi-O nanostructure with record-high performance for electrocatalytic hydrogen evolution reaction *J. Am. Chem. Soc.* **140** 9046–50
- [32] Zhang C, Luo Y, Tan J, Yu Q, Yang F, Zhang Z, Yang L, Cheng H-M and Liu B 2020 High-throughput production of cheap mineral-based two-dimensional electrocatalysts for high-current-density hydrogen evolution *Nat. Commun.* **11** 3724
- [33] Zuo C, Zhou F, Zhang G, Zhong L, Ling J, Yang J, Qiu Y and Tao G 2023 An energy-saving support made of silver nanowire aerogel for hydrogen evolution reaction *Cell Rep. Phys. Sci.* **4** 101377
- [34] Li M, Zhu Y, Wang H, Wang C, Pinna N and Lu X 2019 Ni strongly coupled with Mo₂C encapsulated in nitrogen-doped carbon nanofibers as robust bifunctional catalyst for overall water splitting *Adv. Energy Mater.* **9** 1803185
- [35] Yu L *et al* 2018 Ternary Ni_{2(1-x)}Mo_{2x}P nanowire arrays toward efficient and stable hydrogen evolution electrocatalysis under large-current-density *Nano Energy* **53** 492–500
- [36] Du C, Shang M, Mao J and Song W 2017 Hierarchical MoP/Ni₂P heterostructures on nickel foam for efficient water splitting *J. Mater. Chem. A* **5** 15940–9
- [37] Xue S, Liu Z, Ma C, Cheng H-M and Ren W 2020 A highly active and durable electrocatalyst for large current density hydrogen evolution reaction *Sci. Bull.* **65** 123–30
- [38] Ma L *et al* 2016 Self-assembled ultrathin NiCo₂S₄ nanoflakes grown on Ni foam as high-performance flexible electrodes for hydrogen evolution reaction in alkaline solution *Nano Energy* **24** 139–47
- [39] Dong Z, Lin F, Yao Y and Jiao L 2019 Crystalline Ni(OH)₂/amorphous NiMoO mixed-catalyst with Pt-like performance for hydrogen production *Adv. Energy Mater.* **9** 1902703
- [40] Li L, Zou W, Ye Q, Li Q, Feng Q, Wei J, Xu X and Wang F 2021 Quasi-parallel nickel cobalt phosphide nanosheet arrays as highly efficient electrocatalyst for hydrogen evolution and overall water splitting at large current densities *J. Power Sources* **516** 230657
- [41] Yu Z *et al* 2022 MoO_xS_y/Ni₃S₂ microspheres on Ni foam as highly efficient, durable electrocatalysts for hydrogen evolution reaction *Chem. Mater.* **34** 798–808
- [42] Chen Z-J, Cao G-X, Gan L-Y, Dai H, Xu N, Zang M-J, Dai H-B, Wu H and Wang P 2018 Highly dispersed platinum on honeycomb-like NiO@Ni film as a synergistic electrocatalyst for the hydrogen evolution reaction *ACS Catal.* **8** 8866–72
- [43] Song F, Li W, Yang J, Han G, Liao P and Sun Y 2018 Interfacing nickel nitride and nickel boosts both electrocatalytic hydrogen evolution and oxidation reactions *Nat. Commun.* **9** 4531
- [44] Kou T *et al* 2020 Carbon doping switching on the hydrogen adsorption activity of NiO for hydrogen evolution reaction *Nat. Commun.* **11** 590
- [45] Zhang J-Y *et al* 2022 Synthesis of Ni/NiO@MoO₃–Composite nanoarrays for high current density hydrogen evolution reaction *Adv. Energy Mater.* **12** 2200001
- [46] Zhou H *et al* 2016 Efficient hydrogen evolution by ternary molybdenum sulfoselenide particles on self-standing porous nickel diselenide foam *Nat. Commun.* **7** 12765
- [47] Zhao Y, Ling T, Chen S, Jin B, Vasileff A, Jiao Y, Song L, Luo J and Qiao S-Z 2019 Non-metal single-iodine-atom electrocatalysts for the hydrogen evolution reaction *Angew. Chem., Int. Ed.* **58** 12252–7

- [48] Sivanantham A, Ganesan P and Shanmugam S 2016 Hierarchical NiCo₂S₄ nanowire arrays supported on Ni foam: an efficient and durable bifunctional electrocatalyst for oxygen and hydrogen evolution reactions *Adv. Funct. Mater.* **26** 4661–72
- [49] An Y, Long X, Ma M, Hu J, Lin H, Zhou D, Xing Z, Huang B and Yang S 2019 One-step controllable synthesis of catalytic Ni₄Mo/MoO/Cu nanointerfaces for highly efficient water reduction *Adv. Energy Mater.* **9** 1901454
- [50] Hu J, Li S, Li Y, Wang J, Du Y, Li Z, Han X, Sun J and Xu P 2020 A crystalline-amorphous Ni-Ni(OH)₂core-shell catalyst for the alkaline hydrogen evolution reaction *J. Mater. Chem. A* **8** 23323–9
- [51] Li Y, Tan X, Hocking R K, Bo X, Ren H, Johannessen B, Smith S C and Zhao C 2020 Implanting Ni-O-VO_x sites into Cu-doped Ni for low-overpotential alkaline hydrogen evolution *Nat. Commun.* **11** 2720
- [52] Tan Y *et al* 2021 Facile fabrication of robust hydrogen evolution electrodes under high current densities via Pt@Cu interactions *Adv. Funct. Mater.* **31** 2105579
- [53] Song C, Zhao Z, Sun X, Zhou Y, Wang Y and Wang D 2019 *In situ* growth of Ag nanodots decorated Cu₂O porous nanobelts networks on copper foam for efficient HER electrocatalysis *Small* **15** 1804268
- [54] Yu J, Li G, Liu H, Zeng L, Zhao L, Jia J, Zhang M, Zhou W, Liu H and Hu Y 2019 Electrochemical flocculation integrated hydrogen evolution reaction of Fe@N-doped carbon nanotubes on iron foam for ultralow voltage electrolysis in neutral media *Adv. Sci.* **6** 1901458
- [55] Lv H, Fu C, Fan J, Zhang Y and Hao W 2022 Mild construction of robust FeS-based electrode for pH-universal hydrogen evolution at industrial current density *J. Colloid Interface Sci.* **626** 384–94
- [56] Zhang X-Y, Li F-T, Fan R-Y, Zhao J, Dong B, Wang F-L, Liu H-J, Yu J-F, Liu C-G and Chai Y-M 2021 F, P double-doped Fe₃O₄ with abundant defect sites for efficient hydrogen evolution at high current density *J. Mater. Chem. A* **9** 15836–45
- [57] Cui T, Zhai X, Guo L, Chi J-Q, Zhang Y, Zhu J, Sun X and Wang L 2022 Controllable synthesis of a self-assembled ultralow Ru, Ni-doped Fe₂O₃ lily as a bifunctional electrocatalyst for large-current-density alkaline seawater electrolysis *Chin. J. Catal.* **43** 2202–11
- [58] Zhang L, Liang Q, Huang Y, Li H, Zhou M, He B, Liu Y, Yang H and Yan J 2018 Microspheric flower-like Co₄S₃@Co foam synthesized by *in situ* sulfidization for electrocatalytic hydrogen evolution reaction *J. Mater. Sci., Mater. Electron.* **29** 19336–43
- [59] Sun H, Ma Z, Qiu Y, Liu H and Gao G-G 2018 Ni@NiO nanowires on nickel foam prepared via “acid hungry” strategy: high supercapacitor performance and robust electrocatalysts for water splitting reaction *Small* **14** 1800294
- [60] Zuo Z, Zhang X, Peng O, Shan L, Xiang S, Lian Q, Li N, Mi G, Amini A and Cheng C 2024 Self-supported iron-based bimetallic phosphide catalytic electrode for efficient hydrogen evolution reaction at high current density *J. Mater. Chem. A* **12** 5331–9
- [61] Pei Y, Huang L, Han L, Zhang H, Dong L, Jia Q and Zhang S 2022 NiCoP/NiOOH nanoflowers loaded on ultrahigh porosity Co foam for hydrogen evolution reaction under large current density *Green Energy Environ.* **7** 467–76
- [62] Huang J-F and Wu Y-C 2018 Making Ag present Pt-like activity for hydrogen evolution reaction *ACS Sustain. Chem. Eng.* **6** 8285–90
- [63] Yang M, Zhang Y, Jian J, Fang L, Li J, Fang Z, Yuan Z, Dai L, Chen X and Yu D 2019 Donor-acceptor nanocarbon ensembles to boost metal-free all-pH hydrogen evolution catalysis by combined surface and dual electronic modulation *Angew. Chem., Int. Ed.* **58** 16217–22
- [64] Li C *et al* 2022 Ultrafast self-heating synthesis of robust heterogeneous nanocarbides for high current density hydrogen evolution reaction *Nat. Commun.* **13** 3338
- [65] Li X, Wang Y, Wang J, Da Y, Zhang J, Li L, Zhong C, Deng Y, Han X and Hu W 2020 Sequential electrodeposition of bifunctional catalytically active structures in MoO₃/Ni-NiO composite electrocatalysts for selective hydrogen and oxygen evolution *Adv. Mater.* **32** 2003414
- [66] Zhang Y, Ouyang B, Xu J, Chen S, Rawat R S and Fan H J 2016 3D prous hierarchical nickel–molybdenum nitrides synthesized by RF plasma as highly active and stable hydrogen-evolution-reaction electrocatalysts *Adv. Energy Mater.* **6** 1600221
- [67] Zhai L, Benedict Lo T W, Xu Z-L, Potter J, Mo J, Guo X, Tang C C, Edman Tsang S C and Lau S P 2020 *In situ* phase transformation on nickel-based selenides for enhanced hydrogen evolution reaction in alkaline medium *ACS Energy Lett.* **5** 2483–91
- [68] Jing F, Du S, Ding Z, Chen X, Liu Z and Mei H 2024 N-doped NiS₂ nanosheets array on carbon fiber as an efficient hydrogen evolution reaction electrocatalyst *Transit. Met. Chem.* **49** 429–37
- [69] Lv X, Wan S, Mou T, Han X, Zhang Y, Wang Z and Tao X 2023 Atomic-level surface engineering of nickel phosphide nanoarrays for efficient electrocatalytic water splitting at large current density *Adv. Funct. Mater.* **33** 2205161
- [70] Yang F *et al* 2022 Fabrication of robust CoP/Ni₂P/CC composite for efficient hydrogen evolution reaction and the reduction of graphene oxide *Int. J. Hydrog. Energy* **47** 20448–61
- [71] Zhou K, Zhang Q, Wang Z, Wang C, Han C, Ke X, Zheng Z, Wang H, Liu J and Yan H 2019 A Setaria-inflorescence-structured catalyst based on nickel-cobalt wrapped silver nanowire conductive networks for highly efficient hydrogen evolution *J. Mater. Chem. A* **7** 26566–73
- [72] Guo R, Shi J, Hong L, Ma K, Zhu W, Yang H, Wang J, Wang H and Sheng M 2022 CoP₂/Co₂P encapsulated in carbon nanotube arrays to construct self-supported electrodes for overall electrochemical water splitting *ACS Appl. Mater. Interfaces* **14** 56847–55
- [73] Kumar A, Bui V Q, Lee J, Jadhav A R, Hwang Y, Kim M G, Kawazoe Y and Lee H 2021 Modulating interfacial charge density of NiP₂-FeP₂ via coupling with metallic Cu for accelerating alkaline hydrogen evolution *ACS Energy Lett.* **6** 354–63
- [74] Hoa V H, Prabhakaran S, Nhi Le K T and Kim D H 2022 A single atom Ir doped heterophase of a NiMoP-NiMoP_xO_y ultrathin layer assembled on CNTs-graphene for high-performance water splitting *J. Mater. Chem. A* **10** 14604–12
- [75] Liu W, Wang X, Wang F, Du K, Zhang Z, Guo Y, Yin H and Wang D 2021 A durable and pH-universal self-standing MoC–Mo₂C heterojunction electrode for efficient hydrogen evolution reaction *Nat. Commun.* **12** 6776
- [76] Xie Y *et al* 2019 Boosting water dissociation kinetics on Pt-Ni nanowires by N-induced orbital tuning *Adv. Mater.* **31** 1807780
- [77] Wang X-D, Xu Y-F, Rao H-S, Xu W-J, Chen H-Y, Zhang W-X, Kuang D-B and Su C-Y 2016 Novel porous molybdenum tungsten phosphide hybrid nanosheets on carbon cloth for efficient hydrogen evolution *Energy Environ. Sci. Adv.* **9** 1468–75
- [78] Chen J, Ha Y, Wang R, Liu Y, Xu H, Shang B, Wu R and Pan H 2022 Inner Co synergizing outer Ru supported on

- carbon nanotubes for efficient pH-universal hydrogen evolution catalysis *Nano-Micro Lett.* **14** 186
- [79] Gu Y, Chen S, Ren J, Jia Y A, Chen C, Komarneni S, Yang D and Yao X 2018 Electronic structure tuning in Ni₃FeN/r-GO aerogel toward bifunctional electrocatalyst for overall water splitting *ACS Nano* **12** 245–53
- [80] Gong M *et al* 2014 Nanoscale nickel oxide/nickel heterostructures for active hydrogen evolution electrocatalysis *Nat. Commun.* **5** 4695
- [81] Riyajuddin S, Azmi K, Pahuja M, Kumar S, Maruyama T, Bera C and Ghosh K 2021 Super-hydrophilic hierarchical Ni-foam-graphene-carbon nanotubes-Ni₂P-CuP₂ nano-architecture as efficient electrocatalyst for overall water splitting *ACS Nano* **15** 5586–99
- [82] Murthy A P, Madhavan J and Murugan K 2018 Recent advances in hydrogen evolution reaction catalysts on carbon/carbon-based supports in acid media *J. Power Sources* **398** 9–26
- [83] Zhan J, Cao X, Zhou J, Xu G, Lei B and Wu M 2021 Porous array with CoP nanoparticle modification derived from MOF grown on carbon cloth for effective alkaline hydrogen evolution *Chem. Eng. J.* **416** 128943
- [84] Sun J, Guo F, Ai X, Tian Y, Yang J, Zou X and Zhu G 2024 Constructing heterogeneous interface by growth of carbon nanotubes on the surface of MoB₂ for boosting hydrogen evolution reaction in a wide pH range *Small* **20** 2304573
- [85] Wang C *et al* 2024 Octahedral nanocrystals of Ru-doped PtFeNiCuW/CNTs high-entropy alloy: high performance toward pH-universal hydrogen evolution reaction *Adv. Mater.* **36** 2400433
- [86] Zhang J, Zhang L, Liu J, Zhong C, Tu Y, Li P, Du L, Chen S and Cui Z 2022 OH spectator at IrMo intermetallic narrowing activity gap between alkaline and acidic hydrogen evolution reaction *Nat. Commun.* **13** 5497
- [87] Li J-S, Wang Y, Liu C-H, Li S-L, Wang Y-G, Dong L-Z, Dai Z-H, Li Y-F and Lan Y-Q 2016 Coupled molybdenum carbide and reduced graphene oxide electrocatalysts for efficient hydrogen evolution *Nat. Commun.* **7** 11204
- [88] Li Z *et al* 2019 *In situ* formed Pt₃Ti nanoparticles on a two-dimensional transition metal carbide (MXene) used as efficient catalysts for hydrogen evolution reactions *Nano Lett.* **19** 5102–8
- [89] Wang T, Zhang D, Fei J, Yu W, Zhu J, Zhang Y, Shi Y, Tian M, Lai J and Wang L 2024 Sub-nanometric Pt clusters supported Co aerogel electrocatalyst with hierarchical micro/nano-porous structure for hydrogen evolution reaction *Appl. Catal. B* **343** 123546
- [90] Zhou K L, Wang Z, Han C B, Ke X, Wang C, Jin Y, Zhang Q, Liu J, Wang H and Yan H 2021 Platinum single-atom catalyst coupled with transition metal/metal oxide heterostructure for accelerating alkaline hydrogen evolution reaction *Nat. Commun.* **12** 3783
- [91] Zheng Y, Li N, Mukherjee S, Yang Y, Yan J, Liu J and Fang Y 2019 A versatile strategy for tailoring noble metal supramolecular gels/aerogels and their application in hydrogen evolution *ACS Appl. Nano Mater.* **2** 3012–20
- [92] Liu Y, Liang X, Gu L, Zhang Y, Li G-D, Zou X and Chen J-S 2018 Corrosion engineering towards efficient oxygen evolution electrodes with stable catalytic activity for over 6000 hours *Nat. Commun.* **9** 2609
- [93] Hao W, Ma X, Wang L, Guo Y, Bi Q, Fan J, Li H and Li G 2024 Surface corrosion-resistant and multi-scenario MoNiP electrode for efficient industrial-scale seawater splitting *Adv. Energy Mater.* **2403009**
- [94] Zhou Y-N, Wang F-L, Nan J, Dong B, Zhao H-Y, Wang F-G, Yu N, Luan R-N, Liu D-P and Chai Y-M 2022 High-density ultrafine RuP₂ with strong catalyst-support interaction driven by dual-ligand and tungsten-oxygen sites for hydrogen evolution at 1 A cm⁻² *Appl. Catal. B* **304** 120917
- [95] Chen Z-N *et al* 2024 Mechanically generating active nickel surface for promoting hydrogen evolution reaction *Acta Mater.* **263** 119522
- [96] Zhang X, Wang J, Wang J, Wang J, Wang C and Lu C 2021 Freestanding surface disordered NiCu solid solution as ultrastable high current density hydrogen evolution reaction electrode *J. Phys. Chem. Lett.* **12** 11135–42
- [97] Qiu Y, Liu S, Wei C, Fan J, Yao H, Dai L, Wang G, Li H, Su B and Guo X 2022 Synergistic effect between platinum single atoms and oxygen vacancy in MoO₂ boosting pH-universal hydrogen evolution reaction at large current density *Chem. Eng. J.* **427** 131309
- [98] Wu L, Yu L, Zhang F, McElhenny B, Luo D, Karim A, Chen S and Ren Z 2021 Heterogeneous bimetallic phosphide Ni₂P-Fe₂P as an efficient bifunctional catalyst for water/seawater splitting *Adv. Funct. Mater.* **31** 2006484
- [99] Chen Y *et al* 2020 Metallic Ni₃Mo₃N porous microrods with abundant catalytic sites as efficient electrocatalyst for large current density and superstability of hydrogen evolution reaction and water splitting *Appl. Catal. B* **272** 118956
- [100] Wang F *et al* 2022 Robust porous WC-based self-supported ceramic electrodes for high current density hydrogen evolution reaction *Adv. Sci.* **9** 2106029
- [101] Zhang J, Shang X, Ren H, Chi J, Fu H, Dong B, Liu C and Chai Y 2019 Modulation of inverse spinel Fe₃O₄ by phosphorus doping as an industrially promising electrocatalyst for hydrogen evolution *Adv. Mater.* **31** 1905107
- [102] Wang Z *et al* 2021 Manipulation on active electronic states of metastable phase β-NiMoO₄ for large current density hydrogen evolution *Nat. Commun.* **12** 5960
- [103] Chen Y *et al* 2017 Highly active, nonprecious electrocatalyst comprising borophene subunits for the hydrogen evolution reaction *J. Am. Chem. Soc.* **139** 12370–3
- [104] Chen X *et al* 2021 Layered Ni-Co-P electrode synthesized by CV electrodeposition for hydrogen evolution at large currents *ChemCatChem* **13** 3619–27
- [105] Zhang X-Y, Li F-T, Zhao J, Dong B, Wang F-L, Wu Z-X, Wang L, Chai Y-M and Liu C-G 2022 Tailoring the D-band centers of FeP nanobelt arrays by fluorine doping for enhanced hydrogen evolution at high current density *Fuel* **316** 123206
- [106] Yang H, Chen Z, Guo P, Fei B and Wu R 2020 B-doping-induced amorphization of LDH for large-current-density hydrogen evolution reaction *Appl. Catal. B* **261** 118240
- [107] Zhang X-Y *et al* 2020 Hydrogen evolution under large-current-density based on fluorine-doped cobalt-iron phosphides *Chem. Eng. J.* **399** 125831
- [108] Zheng Z *et al* 2020 Boosting hydrogen evolution on MoS₂ via co-confining selenium in surface and cobalt in inner layer *Nat. Commun.* **11** 3315
- [109] Jin J *et al* 2021 Atomic sulfur filling oxygen vacancies optimizes H absorption and boosts the hydrogen evolution reaction in alkaline media *Angew. Chem., Int. Ed.* **60** 14117–23
- [110] Zhang X-Y, Wang F-L, Fu J-Y, Zhen Y-N, Dong B, Zhou Y-N, Liu H-J, Liu D-P, Liu C-G and Chai Y-M 2021 Amorphous-crystalline catalytic interface of CoFeOH/CoFeP with double sites based on ultrafast hydrolysis for hydrogen evolution at high current density *J. Power Sources* **507** 230279
- [111] Wu X *et al* 2021 Solvent-free microwave synthesis of ultra-small Ru-Mo₂C@CNT with strong metal-support interaction for industrial hydrogen evolution *Nat. Commun.* **12** 4018

- [112] Hu Q, Gao K, Wang X, Zheng H, Cao J, Mi L, Huo Q, Yang H, Liu J and He C 2022 Subnanometric Ru clusters with upshifted D band center improve performance for alkaline hydrogen evolution reaction *Nat. Commun.* **13** 3958
- [113] Wang L, Hao Y, Deng L, Hu F, Zhao S, Li L and Peng S 2022 Rapid complete reconfiguration induced actual active species for industrial hydrogen evolution reaction *Nat. Commun.* **13** 5785
- [114] Zhang X-Y, Li F-T, Shi Z-N, Dong B, Dong Y-W, Wu Z-X, Wang L, Liu C-G and Chai Y-M 2022 Vanadium doped FeP nanoflower with optimized electronic structure for efficient hydrogen evolution *J. Colloid Interface Sci.* **615** 445–55
- [115] Lin F, Dong Z, Yao Y, Yang L, Fang F and Jiao L 2020 Electrocatalytic hydrogen evolution of ultrathin Co-Mo₅N₆ heterojunction with interfacial electron redistribution *Adv. Energy Mater.* **10** 2002176
- [116] Yao R, Sun K, Zhang K, Wu Y, Du Y, Zhao Q, Liu G, Chen C, Sun Y and Li J 2024 Stable hydrogen evolution reaction at high current densities via designing the Ni single atoms and Ru nanoparticles linked by carbon bridges *Nat. Commun.* **15** 2218
- [117] Wang P, Zhang X, Zhang J, Wan S, Guo S, Lu G, Yao J and Huang X 2017 Precise tuning in platinum-nickel/nickel sulfide interface nanowires for synergistic hydrogen evolution catalysis *Nat. Commun.* **8** 14580
- [118] Feng J-X, Wu J-Q, Tong Y-X and Li G-R 2018 Efficient hydrogen evolution on Cu nanodots-decorated Ni₃S₂ nanotubes by optimizing atomic hydrogen adsorption and desorption *J. Am. Chem. Soc.* **140** 610–7
- [119] Mardle P, Chen B and Holdcroft S 2023 Opportunities of ionomer development for anion-exchange membrane water electrolysis *ACS Energy Lett.* **8** 3330–42
- [120] Klingenhof M *et al* 2024 High-performance anion-exchange membrane water electrolyzers using NiX (X = Fe, Co, Mn) catalyst-coated membranes with redox-active Ni–O ligands *Nat. Catal.* **7** 1213–22
- [121] Li N, Araya S S and Kær S K 2019 Long-term contamination effect of iron ions on cell performance degradation of proton exchange membrane water electrolyser *J. Power Sources* **434** 226755
- [122] Zhang X-L *et al* 2023 Efficient acidic hydrogen evolution in proton exchange membrane electrolyzers over a sulfur-doped marcasite-type electrocatalyst *Sci. Adv.* **9** eadh2885
- [123] Gao L *et al* 2023 Engineering a local potassium cation concentrated microenvironment toward the ampere-level current density hydrogen evolution reaction *Energy Environ. Sci.* **16** 285–94
- [124] Kim H, Park H, Oh S and Kim S-K 2020 Facile electrochemical preparation of nonprecious Co-Cu alloy catalysts for hydrogen production in proton exchange membrane water electrolysis *Int. J. Energy Res.* **44** 2833–44
- [125] Xie Z *et al* 2021 Ultrathin platinum nanowire based electrodes for high-efficiency hydrogen generation in practical electrolyzer cells *Chem. Eng. J.* **410** 128333
- [126] Galyamin D *et al* 2023 Insights into the high activity of ruthenium phosphide for the production of hydrogen in proton exchange membrane water electrolyzers *Adv. Energy Sustain. Res.* **4** 2300059
- [127] Choi K J, Kim H and Kim S-K 2021 Multicomponent nonprecious hydrogen evolution catalysts for high performance and durable proton exchange membrane water electrolyzer *J. Power Sources* **506** 230200
- [128] Ampurdanes J, Chourashiya M and Urakawa A 2019 Cobalt oxide-based materials as non-PGM catalyst for HER in PEM electrolysis and *in situ* XAS characterization of its functional state *Catal. Today* **336** 161–8
- [129] King L A, Hubert M A, Capuano C, Manco J, Danilovic N, Valle E, Hellstern T R, Ayers K and Jaramillo T F 2019 A non-precious metal hydrogen catalyst in a commercial polymer electrolyte membrane electrolyser *Nat. Nanotechnol.* **14** 1071–4
- [130] Wang Y, Zhang M, Kang Z, Shi L, Shen Y, Tian B, Zou Y, Chen H and Zou X 2023 Nano-metal diborides-supported anode catalyst with strongly coupled TaO_x/IrO₂ catalytic layer for low-iridium-loading proton exchange membrane electrolyzer *Nat. Commun.* **14** 5119
- [131] Shi H, Qian J and Hu X 2024 Polyaniline nanowires decorated nickel phosphides hollow spheres hydrogen evolution catalyst for proton exchange membrane electrolysis *J. Power Sources* **596** 234099
- [132] Shen L, Shi Y, Ogundipe T O, Huang K, Cao S, Lu Z, Wang Z, Tan H and Yan C 2022 Hierarchical WMoC nano array with optimal crystal facet as a non-noble metal cathode for proton exchange membrane water electrolyser *J. Power Sources* **538** 231557
- [133] Xie L, Wang L, Liu X, Chen J, Wen X, Zhao W, Liu S and Zhao Q 2024 Flexible tungsten disulfide superstructure engineering for efficient alkaline hydrogen evolution in anion exchange membrane water electrolyzers *Nat. Commun.* **15** 5702
- [134] Son H-J, Hwang J, Choi M Y, Park S H, Jang J H, Han B and Ahn S H 2024 Practical operating flexibility of a bifunctional freestanding membrane for efficient anion exchange membrane water electrolysis across all current ranges *Carbon Energy* **6** e542
- [135] Liang Z, Shen D, Wei Y, Sun F, Xie Y, Wang L and Fu H 2024 Modulating the electronic structure of cobalt-vanadium bimetal catalysts for high-stable anion exchange membrane water electrolyzer *Adv. Mater.* **36** 2408634
- [136] Li Z *et al* 2024 Seed-assisted formation of NiFe anode catalysts for anion exchange membrane water electrolysis at industrial-scale current density *Nat. Catal.* **7** 944–52
- [137] Fu H Q *et al* 2022 Hydrogen spillover-bridged volmer/tafel processes enabling ampere-level current density alkaline hydrogen evolution reaction under low overpotential *J. Am. Chem. Soc.* **144** 6028–39
- [138] Wan L, Xu Z, Xu Q, Wang P and Wang B 2022 Overall design of novel 3D-ordered MEA with drastically enhanced mass transport for alkaline electrolyzers *Energy Environ. Sci. Adv.* **15** 1882–92
- [139] Zhao Y, Sun M, Wen Q, Wang S, Han S, Huang L, Cheng G, Liu Y and Yu L 2022 Homologous NiCoP@NiFeP heterojunction array achieving high-current hydrogen evolution for alkaline anion exchange membrane electrolyzers *J. Mater. Chem. A* **10** 10209–18
- [140] Lin X *et al* 2024 Alleviating OH blockage on the catalyst surface by the puncture effect of single-atom sites to boost alkaline water electrolysis *J. Am. Chem. Soc.* **146** 4883–91
- [141] Kim J-C, Kim J, Park J C, Ahn S H and Kim D-W 2021 Ru₂P nanofibers for high-performance anion exchange membrane water electrolyzer *Chem. Eng. J.* **420** 130491
- [142] Zheng Y *et al* 2024 Anion exchange membrane water electrolysis at 10 A · cm⁻² over 800 hours *Angew. Chem., Int. Ed.* **64** e202413698